JOURNAL OF GEOPHYSICAL RESEARCH, VOL. 99, NO. B6, PAGES 11,623–11,642, JUNE 10, 1994

Seismic signature and geochemistry of an island arc: A multidisciplinary study of the Kohistan accreted terrane, northern Pakistan

D. Jay Miller[1] and Nikolas I. Christensen

Department of Earth and Atmospheric Sciences, Purdue University, West Lafayette, Indiana

Abstract. Systematic sampling and mapping in the Kohistan accreted arc terrane of northern Pakistan has provided a sample suite representing the lithologic diversity of the section from its base along the Main Mantle Thrust upward through several stacked intrusions and their metamorphosed equivalents into the Kohistan batholith. A new lithologic column for the terrane has been developed during the course of this study using geothermobarometry based on elemental exchange reactions calculated from electron microprobe analyses of mineral assemblages. The pressures calculated from the chemical analyses of various mineral assemblages are constrained by recently published activity-composition models and an internally consistent thermodynamic data base. Compressional and shear wave velocities and densities have been measured on samples that represent the diverse lithologies in this section and have been correlated with the new lithologic column. This data set has been augmented with published compositions and values for the uppermost part of the arc, not sampled in this study. Compressional wave velocities range from 4.3 km s^{-1} in supracrustal volcanogenic sediments to 7.5 km s^{-1} in lower crustal mafic cumulates. Underlying ultramafic rocks with velocities of 8.0 to 8.4 km s^{-1} define a sharp seismic Moho. The strong inflection in the velocity profile to greater than 8.0 km s^{-1} is due to the transition from plagioclase-bearing to plagioclase-free cumulate rocks in a continuous ultramafic-mafic intrusion. The base of the crust lies at least four kilometers below this transition. Correlation of these laboratory-measured values and the new lithologic column has allowed development of a velocity profile comparable to profiles developed through more conventional field seismic methods. Geochemical indices of fractionation exhibit a reasonable correlation with compressional and shear wave velocities. An estimate of mean crustal *Vp* is remarkably similar to models for other cordilleran terranes at 6.7 plus or minus 0.05 km s^{-1}. An estimate of the bulk chemical composition of the Kohistan terrane does not compare favorably with most published assessments of bulk continental crustal chemical composition, but is significantly more mafic than the latter. The striking resemblance of our reconstructed velocity profile to models generated from field seismic studies not only addresses the veracity of these models, but suggests that the Kohistan arc is a superbly well-preserved analog for other arc terranes.

Introduction

A consensus exists among geologists that the most significant contribution to the volume of continental crust since the Archean has been the accretion of island arcs along convergent plate boundaries. While the development and acceptance of plate tectonic theory has been invaluable in unraveling the complex geometry of island arcs [e.g., *Hamilton*, 1988], and despite myriad and diverse investigations into seismic properties of crustal materials, ambiguities in the interpretation of crustal structure and composition remain. As resolution of seismic data improves, incorporation of these data into petrologically sound interpretations of crustal compositions presents the opportunity of making outstanding strides toward the resolution of these ambiguities. The boundaries between lithospheric plates can be divided, albeit grossly simplistically, into three general types: transform, divergent, and convergent boundaries. Marked by the development of deep trenches as one plate dives beneath another, and by arcuate volcanic chains along the leading edge of the overriding plate, convergent boundaries are likely to be the most complex and least understood of these margins. Inasmuch as at least 25% of the bulk continental crust has been created by accretion of these volcanic arcs at convergent margins [*Taylor and McLennan*, 1981], any model of crustal structure or composition should reflect the importance of this component.

Obducted slices of ocean crust, ophiolites, as well as drilling programs and direct observation of active rifts where exposed either at suboceanic rift axes or at the surface as in Iceland elucidate the development of divergent margins. Although surface phenomena and seismic studies allow for interpretation of transform boundaries, deformation and steeply dipping structures lead to some ambiguity. Further complications obscure most of the processes involved in the growth and evolution of landforms at convergent boundaries due to the great depths at which these activities occur, depths that generally defy resolution of petrogenetic processes by remote sensing techniques, and

[1]Now at Ocean Drilling Program, College Station, Texas

Paper number 94JB00059.
0148-0227/94/94JB-00059$05.00

are almost invariably inaccessible to direct observation. Since indirect methods of examination of the deep crust can lead to speculation due to complex assemblages of several rock types, a terrane that fortuitously preserves the crust-mantle transition and lower crustal rocks from a volcanic arc even after uplift and exhumation would be of particular significance to geologists. The Kohistan-Ladakh tectonic province of northern Pakistan and northwestern India appears to provide just such a window into rocks that once marked the Moho and the overlying lower crustal cumulates as well as possibly exposing the higher-emplaced differentiates of these lower crustal magma chambers, and the metamorphic equivalents of these cumulates and their differentiates. In this paper we build upon the earlier work of *Chroston and Simmons* [1989] and present a synthetic seismic profile for the Kohistan arc based on the physical properties of a sequence of rocks that represent the major lithologies of this accreted island arc, from its ultramafic cumulate underpinnings through volcaniclastic sediments that overlie and occur as septa between late, shallow crustal granodioritic plutons. We discuss relationships between whole-rock geochemistry and the physical properties of arc related rocks and present a new lithologic column for the Kohistan arc compiled by integrating geobarometric constraints from mineral equilibria and lithologic unit thicknesses from extensive, systematic field mapping. An estimate of the bulk chemical composition of this complete crustal section is derived from whole rock geochemical data and our lithostratigraphic column. We also address the relevance of examining a section with the remarkable continuity and exposure of the Kohistan-Ladakh terrane as it relates to interpretation of the seismic structure of active island arcs worldwide.

Regional Geology

The Kohistan-Ladakh terrane of northern Pakistan and northwestern India has been recognized as a Mesozoic intraoceanic island arc sandwiched between the Asian and Indian plates [*Tahirkheli et al.*, 1980; *Bard et al.*, 1980; *Coward et al.*, 1982] (Figures 1a and 1b). During the Himalayan collision, this arc was partially thrust under the Asian plate and obducted onto the Indian plate. The resulting terrane preserves an outstanding section that has been turned edge up to expose a virtually complete section from its ultramafic underpinnings at the crust/mantle boundary to surface volcanic rocks through the crust of an oceanic island arc.

The arc extends from some distance into Afghanistan northeastward past Gilgit to Nanga Parbat, then southeastward into India, a total distance of more than 600 km, covering an area in excess of 36,000 km^2. The northeast trending anticlinal Nanga Parbat syntaxis nearly bifurcates the terrane, where deep erosion has exposed the underthrusting Indian plate. The Ladakh segment of the arc lies to the east of the Nanga Parbat syntaxis, and the Kohistan segment lies to the west of it. The terrane is bounded on the north by the Main Karakoram Thrust (MKT), alternatively called the northern suture [*Coward et al.*, 1982]. This suture separates the Kohistan arc from the Karakoram Range. The terrane is bounded on the south by the Main Mantle Thrust (MMT), the contact between the Kohistan arc and the Indian plate. To the east and west of the Kohistan arc the MKT and MMT merge to form the Chaman fault and Indus-Tsangpo suture, respectively, where the Asian plate is thrust over the Indian plate.

The main lithologic units of the Kohistan terrane have been recognized by research teams from the United States, United Kingdom, and Pakistan [*Tahirkheli et al.*, 1980; *Bard et al.*, 1980; *Jan and Howie*, 1981; *Coward et al.*, 1982; *Loucks et al.*, 1990; *Treloar et al.*, 1990]. The MKT is characterized by mylonites, greenschists and ophiolitic serpentinites. South of the MKT is the Chalt sedimentary-volcanic supracrustal sequence, that overlies and occurs as septa between plutons of the tonalitic to granodioritic Kohistan batholith. The Kohistan batholith appears to grade downward into a succession of massive diorites and layered gabbros that comprise the Chilas lower-

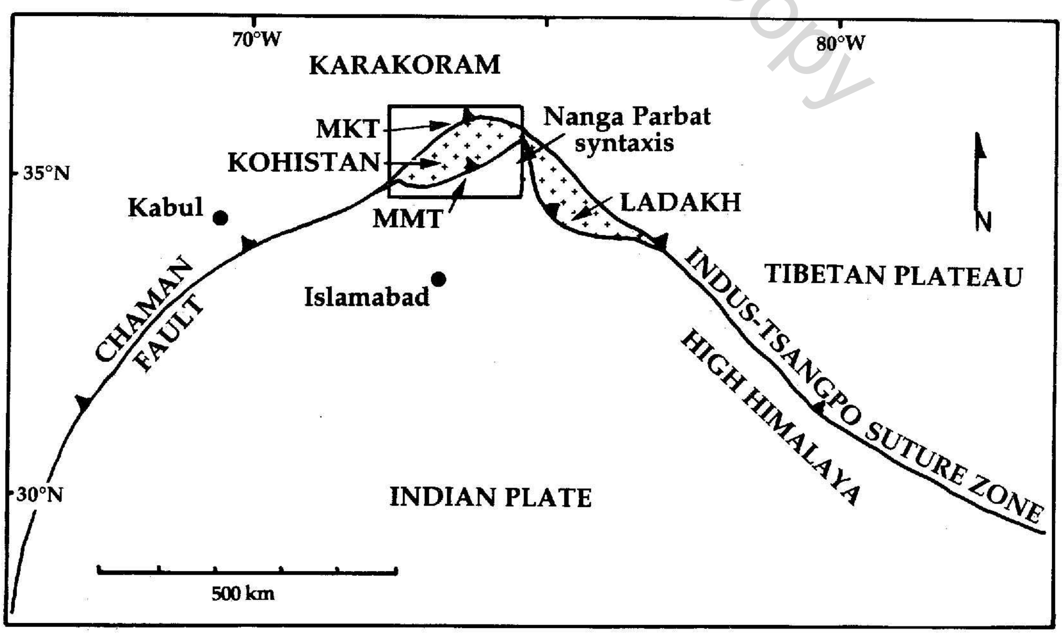

Figure 1a. Sketch map of the Kohistan-Ladakh accreted island arc terrane of northern Pakistan and India. The Main Karakoram Thrust (MKT) and Main Mantle Thrust (MMT) converge west of this terrane into the Chaman Fault, and east into the Indus-Tsangpo suture zone of the high Himalaya (black teeth on overriding plate). Inset box shows location of Figure 1b.

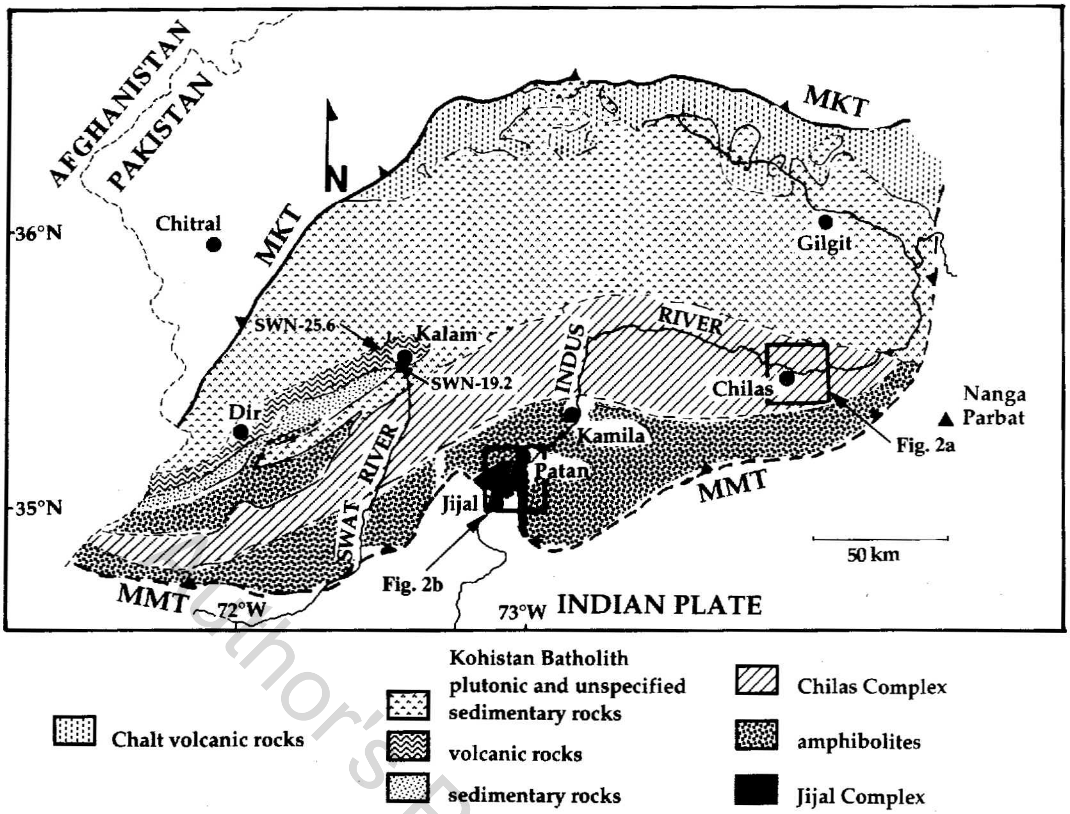

Figure 1b. Simplified geologic map of the Kohistan arc [after *Coward et al.*, 1986, Figure 3], showing recognized lithologic units and boundary faults (black teeth on overriding plate). Inset boxes show locations of Figures 2a and 2b, as well as sample locations off primary traverse lines (near Kalam).

crustal mafic cumulate complex. South of the Chilas Complex is a belt of mafic to dioritic sills and metamorphosed volcanic rocks that have been all grouped into a single unit called the Kamila Amphibolites or alternatively the "Kamila Shear Zone," which has been interpreted as the downfolded equivalents of the Chalt supracrustal sequence to the north that have been overthickened by thrust faulting [*Treloar et al.*, 1990]. South of the Kamila group is the Jijal ultramafic-mafic lower crustal cumulate complex, which comprises the focus of this research. The Jijal Complex is bounded on the south by the MMT, marked in places by a melange of blueschists, greenschists, piedmontite schists and serpentinites presumably derived from the Kohistan arc. These rocks are intermingled with pelitic and quartzofeldspathic schists and gneisses derived from the Indian plate [*Tahirkheli et al.*, 1980; *Bard et al.*, 1980; *Coward et al.*, 1982].

Chroston and Simmons [1989] reported laboratory-measured seismic velocities of samples from, and constructed a seismic velocity model for, the Kohistan arc. Their model was constructed from samples representing the major lithologic units of the terrane. The model of *Chroston and Simmons* [1989] invokes a crustal thickness of 30 km, extracted from the combined work of *Bard et al.* [1980] for the lower part of the section and *Coward et al.* [1982] for the upper part.

Sample Collection, Preparation and Analytical Methods

Two field seasons in 1989 and 1990 were undertaken to assess the geology of the Kohistan arc. Multiple, systematic sampling traverses were made trending perpendicular to the regional strike of the terrane in the Jijal and Chilas complexes (see Figures 2a and 2b). The intervening section of stacked intrusions was sampled during several traverses along the Karakoram Highway (KKH). For the majority of samples, three mutually perpendicular 2.5-cm-long cylindrical cores were extracted in the laboratory by means of a diamond coring bit. Diameters of the cores ranged from 1.25 to 2.5 cm depending upon sample and grain size. If any foliation was present, the primary core was taken normal to it, otherwise, since the samples had no field orientation, the direction of the primary core was randomly chosen. The sample ends were polished to within 0.5° of perpendicular and thin sections were prepared from core ends. The cores were then copper jacketed and sealed with gum rubber to exclude the pressure media. Compressional (*Vp*) and shear (*Vs*) wave velocities were measured using a pulse transmission technique with a mercury delay line [*Birch*, 1960; *Christensen*, 1985]. Velocities were measured at ambient temperatures and at intervals of 20 MPa from 0 to 100 MPa and at 50 MPa intervals from 100 to 600 MPa. Above 10 to 200 MPa, the trend in measured velocity with increasing pressure becomes linear (after microcrack closure). Velocities were measured in 200 MPa increments from 600 to 1000 MPa.

Compressional and shear waves were generated across each sample by means of lead zirconate titanate (PZT) and AC cut quartz transducers with resonant frequencies of 1 MHz. The cumulate error limits for *Vp* and *Vs* are estimated to be less than 1%. Confining pressure was measured by monitoring the change in resistivity of a manganin coil in contact with the pressure media. Densities for each sample were calculated from weights and carefully measured volumes. All measurements were collected and compiled at the Purdue University Rock Physics Laboratory and are tabulated in Table 1.

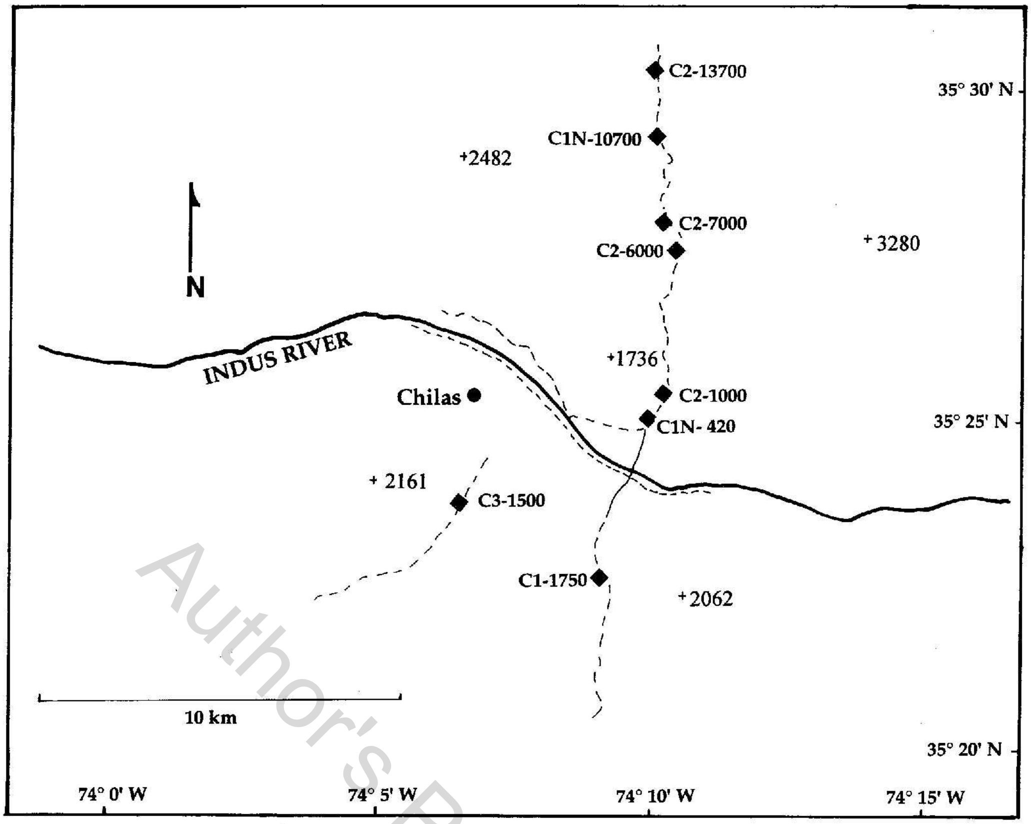

Figure 2a. Traverse lines (dashed) and sample locations (solid diamonds) near Chilas. Pluses mark local topographic highs (elevation in meters above sea level). Indus River altitude in this area is 1000 m.

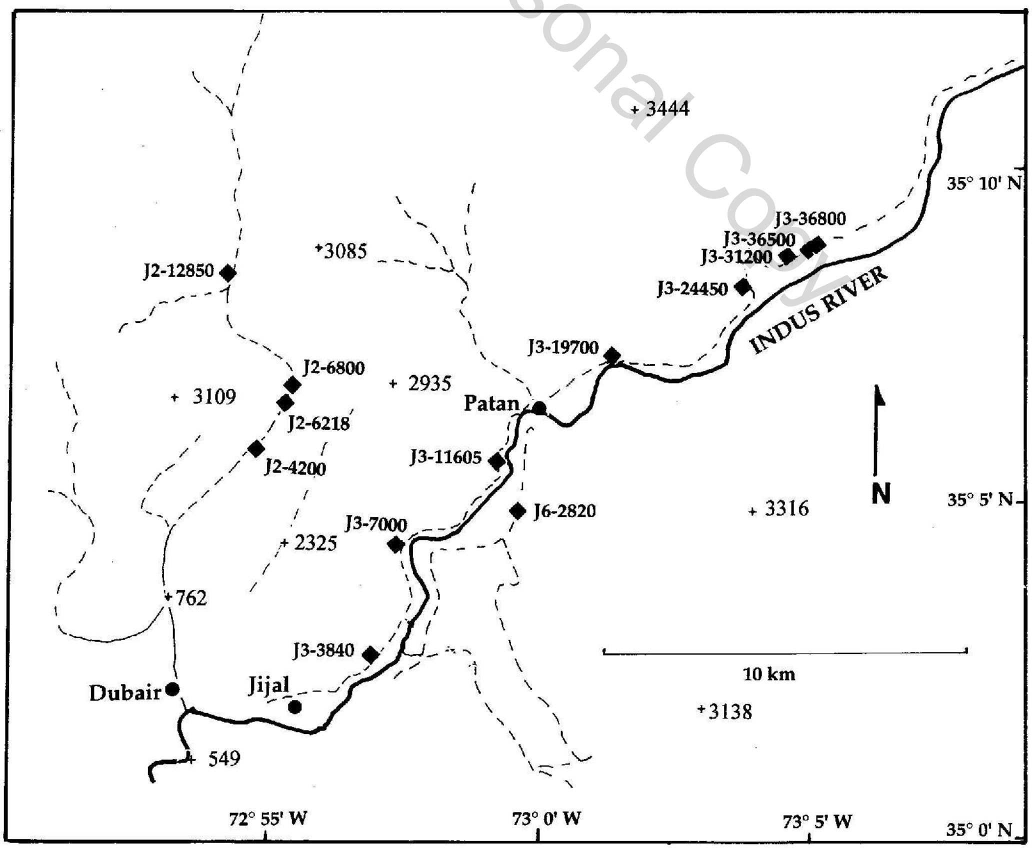

Figure 2b. Traverse lines (dashed) and sample locations (solid diamonds) in the Jijal, Patan, Kayal, and Dasu complexes. Pluses mark local topographic highs (elevation in meters above sea level).

Table 1. Laboratory Measured Densities and Compressional (*Vp*) and Shear (*Vs*) Wave Velocities at Various Confining Pressures for Samples Representing Major Lithologies From the Kohistan Arc

Sample	Core	Density, kg/m^3	P=40 MPa *Vp*	P=40 MPa *Vs*	P=100 MPa *Vp*	P=100 MPa *Vs*	P=200 MPa *Vp*	P=200 MPa *Vs*	P=400 MPa *Vp*	P=400 MPa *Vs*	P=600 MPa *Vp*	P=600 MPa *Vs*	P=1000 MPa *Vp*	P=1000 MPa *Vs*
SWN-26.5	A	2661	5.777	3.433	5.928	3.491	6.053	3.537	6.166	3.576	6.221	3.595	6.285	3.618
SWN-26.5	B	2703	5.838	3.440	6.001	3.515	6.126	3.572	6.235	3.620	6.291	3.644	6.360	3.673
SWN-26.5	Mean	2682	5.808	3.437	5.965	3.504	6.090	3.555	6.201	3.598	6.257	3.620	6.323	3.646
SWN-19.2	A	2912	6.421	3.709	6.569	3.769	6.687	3.814	6.768	3.855	6.796	3.878	6.824	3.908
SWN-19.2	B	2908	6.386	3.719	6.496	3.767	6.585	3.803	6.675	3.837	6.724	3.855	6.781	3.878
SWN-19.2	Mean	2910	6.404	3.715	6.533	3.769	6.637	3.809	6.722	3.846	6.760	3.867	6.803	3.894
C2-13700	A	2896	5.881	3.399	6.252	3.565	6.544	3.680	6.759	3.754	6.845	3.785	6.940	3.821
C2-13700	B	2878	5.884	3.380	6.272	3.540	6.580	3.659	6.824	3.741	6.932	3.774	7.055	3.812
C2-13700	Mean	2887	5.883	3.390	6.262	3.553	6.563	3.670	6.792	3.748	6.889	3.780	6.998	3.817
C1N-10700	A	2938	6.093	3.506	6.137	3.607	6.515	3.654	6.684	3.667	6.753	3.670	6.818	3.673
C1N-10700	B	2982	6.356	3.733	6.632	3.850	6.858	3.941	7.029	4.003	7.098	4.026	7.169	4.051
C1N-10700	C	2980	6.218	3.543	6.560	3.700	6.814	3.812	6.984	3.877	7.048	3.900	7.119	3.925
C1N-10700	Mean	2967	6.223	3.595	6.503	3.720	6.729	3.803	6.900	3.849	6.967	3.866	7.036	3.883
C2-7000	A	2937	6.363	3.586	6.589	3.689	6.772	3.760	6.916	3.805	6.975	3.822	7.038	3.843
C2-7000	B	2943	6.369	3.613	6.612	3.704	6.759	3.769	6.875	3.814	6.940	3.834	7.023	3.857
C2-7000	Mean	2940	6.367	3.600	6.601	3.697	6.766	3.765	6.896	3.810	6.958	3.828	7.031	3.851
C2-6000	A	2784	5.958	3.831	6.106	3.932	6.219	4.008	6.306	4.056	6.346	4.073	6.394	4.091
C2-6000	B	2796	6.014	3.660	6.155	3.721	6.275	3.773	6.377	3.817	6.420	3.836	6.464	3.855
C2-6000	Mean	2790	5.987	3.746	6.131	3.827	6.248	3.891	6.342	3.987	6.384	3.955	6.430	3.973
C2-1000	A	3006	6.813	3.830	6.940	3.879	7.033	3.918	7.118	3.949	7.166	3.962	7.227	3.976
C1N-420	A	3012	7.245	3.997	7.341	4.071	7.414	4.091	7.477	4.903	7.509	4.093	7.549	4.094
C1N-420	B	3031	7.171	4.066	7.358	4.111	7.458	4.135	7.537	4.142	7.581	4.143	7.638	4.143
C1N-420	C	3023	7.310	4.051	7.423	4.141	7.502	4.167	7.575	4.174	7.617	4.178	7.671	4.182
C1N-420	Mean	3022	7.242	4.039	7.375	4.108	7.459	4.131	7.530	4.137	7.570	4.138	7.620	4.140
C3-1500	A	3067	7.275	4.063	7.381	4.097	7.454	4.111	7.516	4.124	7.551	4.131	7.594	4.141
C3-1500	B	3002	6.841	3.879	7.091	3.974	7.231	4.021	7.322	4.048	7.369	4.062	7.429	4.080
C3-1500	C	2997	7.095	3.942	7.227	4.007	7.300	4.047	7.366	4.064	7.404	4.068	7.453	4.071
C3-1500	Mean	3022	7.071	3.962	7.234	4.027	7.329	4.060	7.402	4.079	7.442	4.087	7.493	4.098
C1-1750	A	2977	6.768	3.861	6.917	3.911	7.022	3.947	7.107	3.975	7.151	3.989	7.207	4.007
C1-1750	B	2961	6.687	3.764	6.810	3.807	6.908	3.838	6.993	3.863	7.033	3.876	7.080	3.891
C1-1750	C	2934	6.745	3.755	6.865	3.794	6.697	3.824	7.060	3.851	7.102	3.866	7.145	3.884
C1-1750	Mean	2.957	6.734	3.794	6.854	3.838	6.966	3.870	7.054	3.897	7.096	3.911	7.145	3.928
J3-36800	A	2910	5.142	3.465	5.995	3.775	6.450	3.946	6.637	4.016	6.701	4.038	6.778	4.065
J3-36800	B	2942	6.051	3.606	6.724	3.953	7.174	4.168	7.370	4.259	7.404	4.279	7.431	4.300
J3-36800	C	3036	5.479	3.217	6.050	3.540	6.511	3.777	6.841	3.940	6.691	4.009	7.085	4.090
J3-36800	Mean	3000	5.643	3.242	6.113	3.499	6.506	3.707	6.820	3.876	6.947	3.951	7.080	4.032
J3-36500	A	2882	6.237	3.719	6.476	3.812	6.636	3.867	6.734	3.896	6.775	3.908	6.823	3.923
J3-36500	B	2857	6.237	3.755	6.435	3.828	6.555	3.876	6.633	3.906	6.673	3.918	6.722	3.934
J3-36500	C	2896	6.467	3.784	6.644	3.871	6.762	3.920	6.852	3.952	6.900	3.969	6.961	3.990
J3-36500	Mean	2878	6.314	3.753	6.519	3.837	6.651	3.888	6.740	3.919	6.783	3.932	6.836	3.949
J3-24450	A	2969	5.789	3.387	6.139	3.570	6.449	3.705	6.694	3.794	6.781	3.827	6.854	3.864
J3-24450	B	2971	5.701	3.421	6.138	3.605	6.508	3.743	6.788	3.832	6.889	3.863	6.984	3.896
J3-24450	C	2964	6.107	3.454	6.430	3.603	6.701	3.720	6.894	3.794	6.958	3.818	7.015	3.842
J3-24450	Mean	2968	5.866	3.421	6.236	3.593	6.553	3.723	6.793	3.807	6.876	3.837	6.951	3.868
J3-19700	A	2948	5.923	3.239	6.320	3.629	6.646	3.809	6.912	3.900	7.027	3.945	7.155	4.003
J3-19700	B	2950	4.917	3.149	5.555	3.469	6.066	3.693	6.449	3.844	6.609	3.912	6.788	3.994
J3-19700	C	2916	5.518	3.344	5.964	3.631	6.318	3.826	6.597	3.949	6.722	4.001	6.868	4.064
J3-19700	Mean	2938	4.453	3.244	5.947	3.576	6.344	3.776	6.653	3.898	6.787	3.953	6.937	4.021
J2-12850	A	2997	6.970	3.964	7.214	4.077	7.317	4.147	7.403	4.210	7.454	4.247	7.519	4.295
J3-11605	A	3139	5.972	3.559	6.576	3.848	6.965	4.012	7.186	4.085	7.274	4.109	7.380	4.138
J3-11605	B	3154	6.027	3.642	6.530	3.856	6.907	3.995	7.166	4.066	7.270	4.089	7.388	4.115

Table 1. (continued)

Sample	Core	Density, kg/m³	P=40 MPa Vp	P=40 MPa Vs	P=100 MPa Vp	P=100 MPa Vs	P=200 MPa Vp	P=200 MPa Vs	P=400 MPa Vp	P=400 MPa Vs	P=600 MPa Vp	P=600 MPa Vs	P=1000 MPa Vp	P=1000 MPa Vs
J3-11605	C	3162	6.274	3.624	6.748	3.936	7.021	4.091	7.194	4.157	7.282	4.183	7.392	4.216
J3-11605	Mean	3152	6.092	3.609	6.618	3.880	6.965	4.033	7.182	4.103	7.275	4.128	7.387	4.157
J6-2820	A	3221	6.668	3.877	6.895	4.039	7.218	4.137	7.376	4.194	7.439	4.218	7.510	4.249
J6-2820	B	3204	6.889	4.005	7.129	4.094	7.299	4.159	7.408	4.205	7.452	4.225	7.504	4.248
J6-2820	C	3214	6.700	3.896	7.026	4.042	7.246	4.135	7.384	4.193	7.442	4.219	7.511	4.252
J6-2820	Mean	3213	6.753	3.927	7.047	4.059	7.255	4.144	7.390	4.197	7.445	4.221	7.509	4.250
J2-6800	A	3288	6.460	3.951	7.074	4.219	7.398	4.364	7.575	4.445	7.659	4.485	7.766	4.534
J2-6800	B	3469	7.635	4.310	7.855	4.408	8.017	4.498	8.180	4.579	8.277	4.613	8.400	4.644
J2-6800	C	3238	6.702	3.997	7.086	4.222	7.332	4.352	7.580	4.426	7.730	4.461	7.922	4.504
J2-6800	Mean	3332	6.933	4.087	7.339	4.284	7.583	4.405	7.779	4.484	7.889	4.520	8.030	4.561
J3-6218	A	3320	6.448	3.900	7.142	4.115	7.670	4.287	8.027	4.422	8.162	4.479	8.312	4.543
J3-6218	B	3313	6.353	3.913	7.044	4.150	7.589	4.339	7.938	4.473	8.045	4.524	8.146	4.577
J3-6218	C	3333	6.739	3.977	7.289	4.183	7.720	4.344	8.051	4.487	8.196	4.537	8.363	4.586
J3-6218	Mean	3322	6.514	3.930	7.159	4.150	7.660	4.327	8.006	4.461	8.135	4.514	8.274	4.569
J3-7000	A	3323	7.099	4.159	7.534	4.327	7.773	4.422	7.898	4.481	7.954	4.512	8.024	4.551
J3-7000	B	3337	7.270	4.183	7.710	4.352	7.972	4.440	8.111	4.488	8.168	4.512	8.237	4.541
J3-7000	C	3345	7.310	4.168	7.634	4.323	7.796	4.393	7.897	4.426	7.952	4.442	8.020	4.461
J3-7000	Mean	3335	7.227	4.171	7.626	4.335	7.848	4.419	7.969	4.466	8.025	4.489	8.094	4.518
J2-4200	A	3154	7.737	4.368	7.822	4.392	7.889	4.409	7.948	4.425	7.978	4.435	8.013	4.447
J2-4200	B	3174	7.543	4.216	7.637	4.298	7.702	4.337	7.776	4.359	7.828	4.370	7.902	4.384
J2-4200	C	3184	7.329	4.309	7.403	4.342	7.464	4.369	7.525	4.395	7.558	4.410	7.595	4.428
J2-4200	Mean	3171	7.537	4.298	7.621	4.345	7.686	4.372	7.750	4.394	7.789	4.405	7.837	4.420
J3-3840	A	3299	8.166	4.669	8.262	4.716	8.319	4.745	8.360	4.770	8.382	4.785	8.411	4.804

Whole rock geochemical analyses were acquired from Acme Analytical Laboratories, Vancouver, British Columbia, by inductively coupled plasma (ICP) analyses (for technique, see *Varma* [1991]). Standards were included in the sample set as unknowns to assure the geochemical analyses were within acceptable error limits for each major oxide and trace element. The whole rock major element oxide abundances and calculated normative mineral abundances are presented in Table 2.

The primary controls on compressional and shear wave velocities in the Earth's crust are mineral composition, preferred mineral orientation, temperature, confining pressure, and pore fluid pressure. In order to generate a seismic profile given known mineral compositions and laboratory measured confining pressures, estimates for the contributions to seismic velocities of the other factors must be considered. Temperature effects on seismic velocity have been documented by *Christensen* [1979]. As temperature increases velocity decreases, typically 2.0 to 6.0 x 10^{-4} km s^{-1} °C^{-1} for most rock types. An error in estimation of 200°C in lower crustal temperature results in less than 0.1 km s^{-1} error in seismic velocity for relevant lithologies. Anisotropy effects may be assessed by measuring physical properties on mutually perpendicular cores: however, since most of the samples collected in this study were seismically isotropic, we invoke a seismically isotropic crust in this model. Although pore pressure can significantly lower seismic velocities [e.g., *Christensen*, 1989], this model uses laboratory velocities measured only as a function of confining pressure.

Geochemistry-Velocity Systematics

In that chemical composition is a primary control on velocity behavior, it is appropriate to evaluate, by means of several covariation diagrams, this connection. In Figures 3a-3d we examine the correlation between laboratory measured compressional and shear wave velocities and four geochemical indices commonly invoked as representative of degree of magmatic evolution [*LeMaitre*, 1976; *Cox et al.*, 1979]. One previously recognized relationship is that compressional velocity varies inversely with weight percent SiO_2 [*Christensen and Szymanski*, 1988]. This trend is evident in a plot of velocity versus weight percent SiO_2 of samples from the Kohistan arc (Figure 3a). In detail, however, samples with the same SiO_2 content differ by as much as 1 km s^{-1} in compressional wave velocity. For example, samples J3-3840, C1N-420, and C2-1000 all have 44.0 plus or minus 0.6 weight percent SiO_2, but compressional wave velocity ranges from 8.41 to 7.23 km s^{-1}.

Another geochemical index that shows good correlation with *Vp* and *Vs* is Mg # (calculated as mole proportion Mg divided by mole proportion Mg + mole proportion Fe). Generally decreasing velocities accompany decreasing Mg # (Figure 3b). Inasmuch as this index is a ratio which combines the effects of Mg depletion by crystallization of olivine and pyroxene, and relative Fe enrichment, this correlation is analogous to *Birch's* [1961] relationship between velocity, density, and mean atomic weight.

Petrologists have recognized the usefulness of total alkali content as a lithology discriminant [e.g., *LeMaitre*, 1976; *Cox et al.*, 1979]. For the sample suite from Kohistan, there is also a distinct correlation between laboratory measured *Vp* and *Vs* and total alkalis (Figure 3c). While the covariation between velocity and alkali content exhibits a more compact pattern than present in a velocity-silica content plot, density controls are still apparent. A garnet hornblendite and a gabbronorite both have the same total alkali content (≈ 2 weight percent). Their re-

Table 2. Whole Rock Major Element Analyses and Calculated Normative Mineralogies for Samples Representing Major Lithologies From the Kohistan Arc

	J3-3840	J2-4200	J3-7000	J2-6800	J2-6218	J6-2820	J3-11605	J2-12850	J3-19700	J3-24450	J3-31200	J3-36500	J3-36800	C1-1750	C3-1500	C1N-420	C2-1000	C2-6000	C2-7000	C1N-10700	C2-13700	SWN 19.2	SWN 26.5
												Oxide Wt%											
SiO_2	44.25	49.03	47.95	40.46	40.81	50.05	51.91	40.43	51.99	47.39	47.90	57.43	56.55	49.96	42.62	44.60	43.75	75.71	51.48	47.65	51.6	56.02	67.94
TiO_2	0.02	0.05	0.38	0.78	0.01	0.87	0.78	0.11	0.80	2.02	1.08	0.47	0.62	0.25	0.04	0.10	1.28	0.51	1.08	1.40	0.91	0.65	0.51
Al_2O_3	0.34	1.64	4.67	18.00	20.21	17.95	17.7	1.74	17.45	18.11	18.91	17.88	14.65	17.79	22.61	19.27	19.43	10.56	17.40	18.17	19.42	14.76	14.21
Fe_2O_3*	9.48	5.37	10.08	11.55	9.85	12.73	11.89	9.58	10.15	12.31	12.12	7.18	7.63	8.67	9.94	6.26	10.98	5.22	11.68	11.37	10.30	8.86	5.01
MgO	42.38	23.13	16.61	14.98	15.03	5.33	5.02	35.85	5.66	4.78	5.01	3.03	6.36	9.64	11.57	13.23	9.16	1.69	5.45	6.06	5.02	6.42	1.32
CaO	1.27	17.86	18.90	11.15	10.92	9.42	9.39	1.99	9.92	11.12	10.34	7.74	8.86	10.9	11.75	15.21	12.90	4.54	8.87	9.55	8.79	7.04	2.46
MnO	0.13	0.10	0.18	0.10	0.14	0.20	0.19	0.13	0.17	0.20	0.21	0.12	0.15	0.15	0.12	0.09	0.11	0.06	0.17	0.17	0.16	0.13	0.13
Na_2O	0.05	0.14	0.26	1.67	0.38	2.39	2.42	0.11	2.54	3.35	2.95	4.02	3.02	1.65	0.95	0.55	1.18	0.70	3.07	3.70	3.56	1.82	3.91
K_2O	0.29	0.05	0.24	0.27	0.15	0.45	0.36	0.05	0.30	0.20	0.19	0.41	0.61	0.22	0.37	0.25	0.28	0.65	0.71	0.25	0.15	1.72	3.00
P_2O_5	0.08	0.04	0.03	0.01	0.01	0.13	0.11	0.13	0.16	0.71	0.25	0.16	0.15	0.02	0.01	0.01	0.01	0.12	0.20	0.35	0.24	0.13	0.10
Cr_2O_3	0.66	0.35	0.09	0.02	0.00	0.00	0.00	0.43	0.01	0.00	0.01	0.00	0.00	0.04	0.00	0.12	0.01	0.03	0.00	0.01	0.00	0.04	0.01
H_2O†	1.0	2.1	0.5	0.7	2.4	0.3	0.1	9.3	0.7	0.0	0.9	1.4	1.2	0.6	0.0	0.2	0.6	0.1	0.0	1.1	0.3	2.2	1.2
Total	99.95	99.86	99.89	99.69	99.91	99.82	99.87	99.85	99.85	100.19	99.87	99.84	99.8	99.89	99.98	99.89	99.69	99.89	100.11	99.78	100.45	99.79	99.8
												Normative											
Q	...	...	...	...	...	2.03	5.09	...	6.08	...	...	10.51	8.85	0.77	...	...	...	55.42	2.59	...	2.15	12.75	24.91
Or	1.71	0.30	1.42	1.60	0.89	2.66	2.13	0.30	1.77	1.18	1.12	2.42	3.61	1.30	2.19	1.48	1.65	3.84	4.20	1.48	0.89	10.17	17.73
Ab	0.13	1.18	0.89	0.75	3.22	20.22	20.48	0.93	21.49	28.35	24.96	34.02	25.56	13.96	7.2	3.32	9.99	5.92	25.98	31.31	30.13	15.4	33.09
An	...	3.70	10.87	40.82	52.97	37.06	36.37	4.11	35.46	33.79	37.77	29.59	24.62	40.51	56.31	49.46	46.81	21.74	31.6	32.31	36.51	27.13	11.55
Ne	...	...	...	7.25	...	...	...	...	...	...	...	...	...	...	0.46	0.72	...	...	...	...	...	...	...
Di	4.54	66.72	65.85	11.33	0.83	7.32	7.88	3.86	10.31	13.69	9.58	6.39	14.77	10.79	1.74	20.53	14.52	...	9.07	10.38	4.52	5.60	...
Hy	24.43	1.39	...	...	3.03	23.89	22.02	25.66	16.77	6.24	15.32	10.90	14.94	27.65	...	...	5.09	8.22	18.29	2.56	18.46	20.51	7.25
Ol	62.97	21.57	14.42	30.71	33.08	...	...	49.91	...	5.25	1.06	...	...	...	27.7	21.09	13.83	...	...	11.51	...	...	...
Mt	3.31	1.94	3.67	4.20	2.57	3.32	3.10	4.16	4.68	5.35	5.61	3.33	3.32	3.15	3.61	2.28	4.78	2.78	5.09	4.96	4.48	3.86	2.17
Il	0.04	0.09	0.72	1.48	0.02	1.65	1.48	0.21	1.52	3.84	2.05	0.89	1.18	0.47	0.08	0.19	2.43	0.97	2.05	2.66	1.73	1.23	0.97
Ap	0.19	0.09	0.07	0.02	0.02	0.31	0.26	0.31	0.38	1.68	0.59	0.38	0.36	0.05	0.02	0.02	0.02	0.28	0.47	0.83	0.57	0.31	0.24
Mg #	91.25	90.85	79.15	74.93	77.85	49.09	49.31	91.38	54.02	47.20	48.79	49.30	70.21	71.92	72.84	82.94	65.79	47.80	51.80	55.11	52.91	62.54	37.75
DI	1.85	1.98	3.14	9.70	4.10	26.41	29.06	1.23	28.28	29.53	26.09	47.08	38.91	16.29	10.13	5.60	11.64	65.18	32.48	32.58	32.92	32.92	75.56

*Total iron as Fe_2O_3

†Loss on ignition for ICP analyses

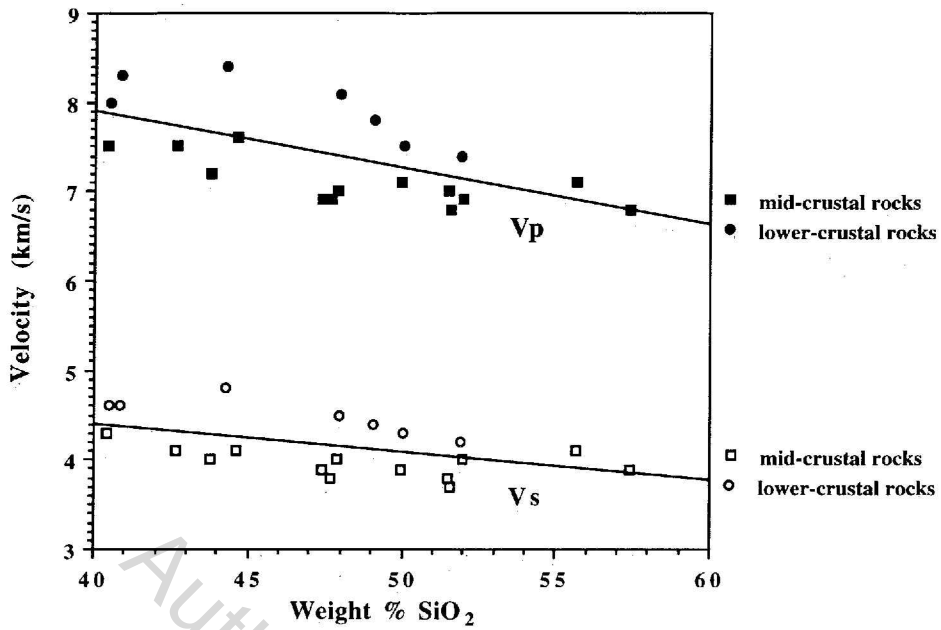

Figure 3a. Laboratory-measured compressional (*Vp*) and shear (*Vs*) wave velocities plotted versus whole rock wt% SiO_2. Lower-crustal rocks represented by samples from the Jijal Complex; midcrustal rocks represented by samples from the Patan, Kayal, Dasu, and Chilas complexes, as well as from the lower part of the Kohistan batholith.

spective densities, however, are 3330 and 2960 kg m^{-3}, and the garnet hornblendite has significantly higher compressional wave velocity.

Statistically, the best correlation between laboratory measured velocities and indicators of fractionation uses the differentiation index (D. I.) of *Thornton and Tuttle* [1960] (Table 3). This is, in effect, a combination of silica and total alkali content as it is based on the abundance of quartz and aluminous alkali silicates calculated from normative abundance. The evidence of density control on velocity behavior is reduced in this plot (Figure 3d). Samples with similar D. I. exhibit just over 0.5 km s^{-1} difference in *Vp*.

Stratigraphy and Seismic Structure

Extensive mapping along multiple traverses roughly perpendicular to the regional strike of the terrane has engendered more rigorous constraints on the lithostratigraphy of the Kohistan arc.

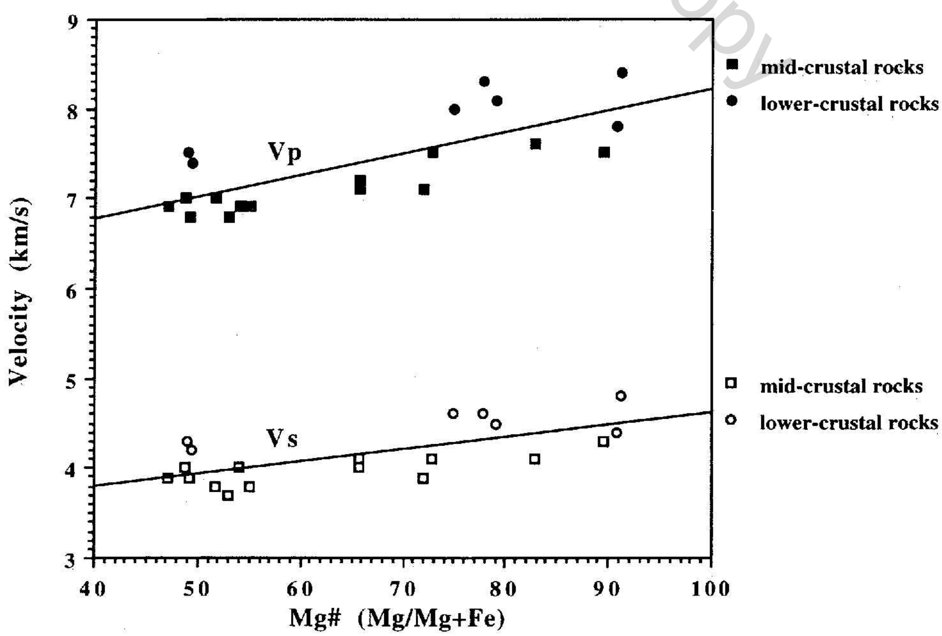

Figure 3b. Laboratory-measured *Vp* and *Vs* plotted versus whole rock magnesium number (mole proportion Mg/mole proportion Mg + mole proportion Fe) Lower-crustal and midcrustal designations are the same as in Figure 3a.

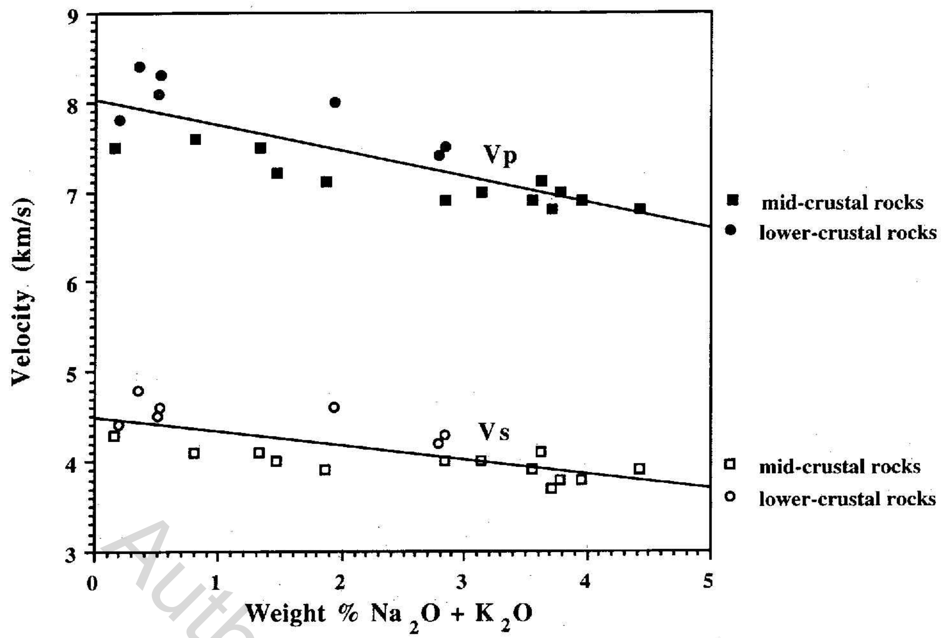

Figure 3c. Laboratory-measured *Vp* and *Vs* plotted versus whole rock wt% Na_2O plus K_2O. Lower-crustal and midcrustal designations are the same as in Figure 3a.

Results of this mapping and subsequent laboratory studies have given rise to several new interpretations, particularly regarding the stratigraphy of the lower part of the section. Two of these interpretations are of principal interest to this research. First, the Jijal Complex is a remarkably well-preserved, layered ultramafic-mafic intrusion. Common igneous textures, graded bedding, scour-and-fill crossbedding, concentrically banded orbicular structures, stratigraphically correlative mineralization and cumulus phase arrivals, as well as a lack of significant late-stage intrusion all suggest that the Jijal Complex was the last in a series of intrusions emplaced at the crust/mantle boundary [*Loucks et al.*, 1990; *Miller et al.*, 1991]. Exhumation of this body through the crust has locally superimposed some metamorphic features, particularly along faulted boundaries, however, much more important, is the recognition of the overwhelming igneous character of this complex. Second, the amphibolite belt between the Jijal and Chilas complexes appears to be a continuous section of at least three more stacked layered intrusions. These intrusions have tentatively been named the Patan, Kayal, and Dasu complexes, for nearby villages. Each is progressively more strongly metamorphosed, with the lowermost Patan Complex preserving unmetamorphosed igneous features and the uppermost Dasu complex exhibiting abundant faulting, folding, and evidence of ductile shearing. In that this research only included mapping from the MMT to the roots of the Kohistan batholith, we rely on published accounts for the upper-

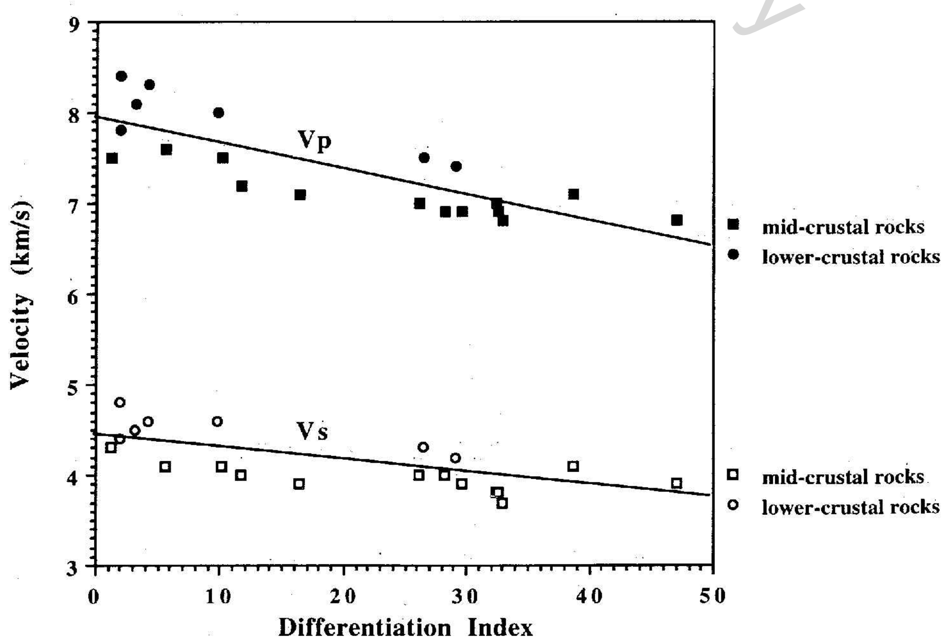

Figure 3d. Laboratory-measured *Vp* and *Vs* plotted versus whole rock Differentiation Index [*Thornton and Tuttle*, 1960]. Lower-crustal and midcrustal designations are the same as in Figure 3a.

Table 3. Least Squares Linear Regression Parameters for Various Geochemical Indices of Fractionation Plotted Against Compressional (*Vp*) and Shear (*Vs*) Wave Velocities.

Vp, km/s	r^2	*Vs*, km/s	r^2
	200 MPa		
10.47–(0.069 x wt % SiO_2)	0.30	5.61–(0.032 x wt % SiO_2)	0.21
5.30+(0.029 x Mg #*)	0.71	3.07+(0.016 x Mg #*)	0.65
7.87–[0.34 x (wt% Na_2O + wt% K_2O)]	0.73	4.44–(0.18 x wt% Na_2O + wt% K_2O)]	0.64
7.82–(0.037 x Differentiation Index†)	0.76	4.40–(0.019 x Differentiation Index†)	0.63
	600 MPa		
10.56–(0.066 x wt % SiO_2)	0.34	5.61–(0.030 x wt % SiO_2)	0.20
5.81+(0.025 x Mg #*)	0.64	3.27+(0.014 x Mg #*)	0.56
8.04–[0.30 x (wt% Na_2O + wt% K_2O)]	0.70	4.50–(0.16 x wt% Na_2O + wt% K_2O)]	0.58
7.98–(0.033 x Differentiation Index†)	0.73	4.46–(0.017 x Differentiation Index†)	0.57
	1000 MPa		
10.66–(0.066 x wt % SiO_2)	0.35	5.60–(0.030 x wt % SiO_2)	0.19
5.95+(0.024 x Mg #*)	0.61	3.33+(0.013 x Mg #*)	0.52
8.10–[0.30 x (wt% Na_2O + wt% K_2O)]	0.68	4.52–(0.16 x wt% Na_2O + wt% K_2O)]	0.55
8.05–(0.032 x Differentiation Index†)	0.71	4.48–(0.016 x Differentiation Index†)	0.54

*Mole proportion Mg/(mole proportion Mg + mole proportion Fe).

†Normative quartz plus all aluminous alkali phases [*Thornton and Tuttle*, 1960].

most part of the arc [*Coward et al.*, 1982; *Jan and Asif*, 1983; *Pudsey*, 1986; *Petterson et al.*, 1991a, b]. For the purposes of reconstruction of the seismic structure of the Kohistan arc, this terrane has been subdivided into five major lithologic units. Locations of samples used in this reconstruction are shown on Figures 2a and b. Petrographic descriptions of these samples are in Table 4.

0-3 km: Volcaniclastic and Sedimentary Rocks

South of the MKT lie the Chalt volcanics. The uppermost rocks from the arc include epidote- and hornblende-bearing tuffs, chlorite schists and amphibolites of volcanic origin. Underlying these are amygdaloidal basalts, basaltic breccia, and intercalated volcanogenic sediments. These are in turn underlain by amygdaloidal pillow lavas and basic schists, intruded by thick gabbroic units. The anomalous thickness of this unit in map view (Figure 1b) is likely due to thrust faulting and repetition of strata [*Coward et al.*, 1982]. Values for the physical properties of the rocks from this part of the arc have been taken from previously reported velocities as a function of pressure [*Christensen*, 1982] for rocks of similar composition. Since the purpose of the current model is to reconstruct the seismic velocity structure of the arc prior to obduction onto the Indian plate, we have used estimated in situ pressures. These values have been selected based on the detailed lithologic descriptions of *Coward et al.* [1982]; *Pudsey* [1986]; *Petterson et al.* [1991a, b].

3-10 km: Tonalite to Diorite Plutons

The next lowest stratigraphic subdivision is the Kohistan batholith. Tonalitic to dioritic in composition, these plutons are quartz-rich and contain plagioclase, mica, and hornblende [*Coward et al.*, 1982; *Jan and Asif*, 1983; *Petterson et al.*, 1991b]. Within these plutons are septa, layers and lenses of metamorphosed volcanogenic sediments represented by samples SWN-26.5 and SWN- 19.2 from this work. *Chroston and Simmons* [1989] tabulate measured velocities for the intrusive rocks in this portion of the arc. The model proposed in this investigation uses worldwide average values for the physical properties of tonalite as compiled by N.I. Christensen (52 samples, unpublished data, 1994). The average density measured by *Chroston and Simmons* [1989] for all the samples from this part of the arc is almost precisely the same as the value used in this model (10 kg m^{-3} difference). The values for *Vp* and *Vs* reported by *Chroston and Simmons* [1989] are both slightly higher than those incorporated into the current model (0.2 and 0.07 km s^{-1}, respectively). Note, however, that *Chroston and Simmons'* [1989] reported values that were all measured at 700 MPa, which corresponds to deep crustal pressures. This new model uses *Vp* and *Vs* values measured at 200-300 MPa, reflecting the estimated depth of crystallization of these plutons. This depth (10 km maximum) is based on geobarometry of the mineral assemblage garnet, rutile, ilmenite, plagioclase, and quartz in the uppermost part of the subjacent lithostratigraphic unit.

10-22 km: Gabbronorite to Diorite Intrusions

This unit is made up of the Chilas ultramafic-mafic complex and the diorites and metadiorites stratigraphically above it that represent the roots of the Kohistan batholith. Geobarometry on samples from the base of the Chilas Complex with the mineral assemblage olivine, plagioclase, clinopyroxene, orthopyroxene, and spinel suggests equilibration (crystallization) pressures of 600-700 MPa. Sample C2-6000 is a fine-grained, quartz-rich rock from the chilled carapace of the intrusion. This model invokes an average pressure of 600 MPa to represent the average equilibration pressure of the entire unit. Values for the mapped dunite in this unit were taken from *Chroston and Simmons* [1989].

22-36 km: Gabbronorite, Metagabbronorite and Amphibolite

These rocks represent the variably metamorphosed amphibolite belt that stretches between the Chilas and Jijal complexes, previously called the Kamila Amphibolites. The uppermost of the three stacked, layered intrusions is the most strongly meta-

Table 4. Petrographic Descriptions of Rocks Representing Major Lithologies From the Kohistan Arc

Sample	Petrography
SWN-26.5	Metadacite (ignimbrite)- contains abundant trachytic lithics, broken, fragmental plagioclase and quartz, a few large skeletal plagioclase crystals, multiphase lithics, several altered pumice fragments. Also contains epidote, chlorite, and rare magnetite.
SWN-19.2	Metaandesite-abundant 2° quartz, primary phenocrysts were plagioclase and clinopyroxene. Little relict plagioclase. A few large pyroxene crystals are preserved, most of sample altered to chlorite + epidote + amphibole + talc.
C2-13700	Diorite-53% plagioclase, 20% clinopyroxene, 10% quartz, with minor hornblende, orthopyroxene, biotite and magnetite. Holocrystalline, adcumulate texture. Medium-coarse-grained. Some hornblende has igneous texture.
C1N-10700	Metadiorite- amphibolitized and strongly foliated. Abundant 2° quartz with epidote, magnetite, and biotite. Plagioclase intensely altered.
C2-7000	Hornblende diorite- 50% plagioclase, 20% clinopyroxene, 10% quartz, 10% hornblende, with orthopyroxene, biotite, and magnetite. Holocrystalline, adcumulate texture. Medium-coarse-grained. Hornblende appears to have igneous texture.
C2-6000	Quartz diorite- Very fine grained, quartz- and hornblende-rich. Chilled margin to Chilas Complex.
C2-1000	Diorite- 40% hornblende, 35% plagioclase, 15% quartz, with orthopyroxene, magnetite, and clinopyroxene. Holocrystalline, very weakly foliated, may be igneous foliation. Medium-fine-grained, but variable in bands parallel to foliation.
C1N-420	Hornblende gabbronorite- 50% plagioclase, 15% hornblende, 15% clinopyroxene, 10% orthopyroxene, 10% quartz. Holocrystalline, adcumulate texture. Medium-coarse-grained. Vermicular intergrowths of minor quartz in hornblende.
C1-1750	Gabbronorite- 60% plagioclase, 20% clinopyroxene, with orthopyroxene, quartz, amphibole, chlorite, and talc. Fairly intensely altered. Medium-grained. Fractured with 2° infilling including calcite and quartz. Plagioclase mildly altered.
C3-1500	Olivine gabbro- 60% plagioclase, 20% olivine, 15% clinopyroxene, with hornblende, spinel, and quartz. Holocrystalline, adcumulate texture. Medium-coarse-grained. Unfoliated. Probably originally troctolite but now contains pyroxene as vermicular intergrowths with spinel and quartz.
J3-36800	Amphibolite- Gneissose. Intensely altered plagioclase, polycrystalline quartz aggregates, abundant rutile, with epidote. Intensely fractured and very strongly foliated.
J3-36500	Amphibolite- Gniessose. Strongly altered plagioclase, polycrystalline quartz common. Very strongly foliated.
J3-31200	Amphibolite- Contains plagioclase, amphibole, epidote, quartz with minor garnet, rutile, ilmenite, and apatite. Medium-coarse-grained. Distinctly foliated. Euhedral epidote and poikiloblastic garnet.
J3-24450	Amphibolite- Contains plagioclase, amphibole, quartz, orthopyroxene with minor ilmenite, apatite, and rutile. Medium-coarse-grained. Moderately to weakly foliated.
J3-19700	Amphibolite- 60% amphibole, 25% plagioclase, 10% quartz,with epidote, rutile, apatite, and ilmenite. Massive, medium-coarse-grained, unfoliated. Complex intergrowths of skeletal amphibole with epidote and quartz.
J2-12850	Serpentinized olivine clinopyroxenite- 70% clinopyroxene, 15% olivine, 15% serpentine. Intensely fractured. Coarse-grained clinopyroxene, medium-fine-grained olivine. Abundant 2° magnetite.
J3-11605	Garnet hornblende gabbro- 30% garnet, 20% plagioclase, 20% quartz, 15% hornblende, 10% clinopyroxene, with minor epidote and rutile. Massive, unfoliated. Medium-coarse-grained. Much of primary pyroxene altered to symplectic amphibole + epidote + quartz.
J6-2820	Garnet gabbro- 35% garnet, 30% plagioclase, 20% clinopyroxene, with quartz, rutile, ilmenite and apatite. Holocrystalline, adcumulate texture. Medium-coarse-grained. Massive, unfoliated. Plagioclase almost completely altered. Garnet euhedral and inclusion free.
J2-6218	Garnet gabbro- 50% garnet, 30% clinopyroxene, 15% plagioclase,with quartz and epidote. Distinctly banded on centimeter scale. Much of clinopyroxene altered to epidote + quartz. Garnet euhedral and inclusion free. Holocrystalline, adcumulate texture.

Table 4. (continued)

Sample	Petrography
J2-6800	Garnet hornblendite- Averages 55% hornblende, 35% garnet but exhibits distinct inch- scale modal banding. Also contains clinopyroxene, ilmenite and rutile. Holocrystalline, adcumulate texture. Coarse-grained. Massive, unfoliated, random fabric.
J3-7000	Websterite- 75% clinopyroxene, 20% orthopyroxene, with chromite, magnetite, and pleonaste. Holocrystalline, adcumulate texture. Coarse-grained. Massive, unfoliated, no preferred mineral orientation.
J2-4200	Wehrlite- 85% clinopyroxene, 15% olivine. Holocrystalline, adcumulate texture. Inch- scale banded. Olivine partially serpentinized.
J3-3840	Chromite dunite- 97% Olivine. Holocrystalline, adcumulate texture. Euhedral-subhedral disseminated chromite. Olivine fresh but shows some evidence of strain in extinction behavior. No texturally evident preferred mineral orientation.

morphosed, and probably the oldest intrusion. This member is underlain by two successively less strongly metamorphosed intrusions. The Patan Complex, in particular, has extensive intervals of well-preserved, massive, igneous cumulate textured rock, as well as unmetamorphosed modally graded layering. This series of intrusions is floored by a thrust fault that separates the Jijal and Patan Complexes. Along one traverse, approximately 3 km of section is missing, but on two others the ultramafic base of the Patan Complex is exposed.

36-45+ km: Ultramafic-Mafic Layered Intrusion

The lowermost section of the crust from this terrane has been the focus of most of this research. The uppermost 5 km of this subdivision are texturally fresh, igneous garnet-bearing gabbros. These are underlain by a chemically contiguous ultramafic cumulate pile. The entire arc is floored by the MMT, the suture between the Indian plate and the Kohistan arc. A few kilometers to the west, the MMT is marked by outcrops of tectonized harzburgite, representing mantle lithologies. The lowermost part of the arc appears to have equilibrated at or near the base of the crust. Sample locations from these units are shown in Figures 2a and 2b. Petrographic descriptions of the samples are in Table 4.

In order to establish the intensive conditions of formation of the stratigraphic units of the Kohistan arc, various geothermobarometers have been constrained by analyzed mineral compositions from representative samples collected during this investigation. Equilibration temperatures were calculated from published ion-exchange geothermometers [*Hakli and Wright*, 1967; *Graham and Powell*, 1984; *Krogh*, 1988; *Blundy and Holland*, 1990] which successfully reproduced temperatures from igneous crystallization experiments [*Carroll and Wyllie*, 1989, 1990; *Brey and Köhler*, 1990]. Recently published mineral solid-solution mixing models and endmember thermodynamic data were applied to pressure dependent mineral equilibria in order to develop a geobarometric profile for the arc. While an explicit exegesis of this method is beyond the scope of this paper, a brief synopsis follows.

After petrographic analysis of more than 200 thin sections representative of the various lithologies sampled, a subset was selected wherein each sample contained a mineral assemblage suitable for geobarometry. To limit the possible effects of subsolidus equilibration of mineral chemistries in these calculations, the subset was reduced by eliminating any samples that exhibited evidence of textural disequilibrium and selecting only the coarsest grained samples. Assuming isobaric crystallization, analyses of the cores of these coarse-grained minerals should record a best estimate of their original compositions. Activity-composition relationships were fixed by recently published, rigorous models for the relevant phases (i.e., plagioclase [*Elkins and Grove*, 1990], garnet [*Berman*, 1990], pyroxene [*Holland*, 1990], and hornblende [*Blundy and Holland*, 1990]. In order to maintain an internally consistent thermodynamic data base for all the phases of interest, the tabulation of *Holland and Powell* [1990] was used in these calculations. Igneous crystallization experiments at high pressure which produced mineral compositions and assemblages similar to the rocks from the Jijal Complex [*Carroll and Wyllie*, 1989, 1990] were used to test the reliability of the geobarometers used in this reconstruction. All reproduced experimental pressures within 100 MPa.

Equilibration pressures for the lowermost lithostratigraphic units of the Kohistan arc are consistent with a geobarometric profile which indicates that the base of the lowermost intrusion crystallized at a depth near 45 km (1450 MPa). Samples from the upper part of the Jijal Complex have mineral compositions indicating equilibration at around 36 km (1200 MPa). The pressure differentials from the lowermost sample containing a geobarometric mineral assemblage through the garnet-bearing mafic sequence are in excellent agreement with the stratigraphic profile generated by field mapping (Table 5). The stratigraphic heights tabulated in Table 5 were estimated by extrapolating structurally oriented samples (based on strike and dip of igneous layering and the first appearance of stratigraphically correlative cumulus minerals) to a hypothetical traverse line perpendicular to the regional strike of the complex. The total calculated pressure differential of 200 MPa is also consistent with the estimated stratigraphic thickness of 6 km for the upper part of the intrusion.

Although geobarometric mineral assemblages are somewhat more rare in rocks from the intrusions stratigraphically above the Jijal Complex, a similarly geologically relevant geobarometric profile from the Chilas Complex indicates equilibration pressures in the lowermost exposed part of this complex of 750-800 MPa (≈22 km) and 500-600 MPa (≈17 km) from the stratigraphically uppermost samples. Integration of the estimated depth of equilibration for the Jijal and Chilas complexes with the extensive mapping program encompassed by this investigation and the observations of published accounts for the uppermost one-third of the arc [*Petterson et al.*, 1991a, b] has allowed

Table 5. Calculated Equilibration Pressures for Stratigraphically Constrained Samples From the Jijal Complex

Approximate Stratigraphic Height, km	Sample	Geobarometer (pressure in MPa)				
		AJQ	GADiS	GAHdS	GAHS	GODSS
9.00	J3-16800	1020	1200	1210	1350	
7.82	J3-14750	1240	1280	1270	1320	
7.60	J3-14456					
6.17	J3-11600	1240	1290	1280	1400	
5.81	J3-10965	1260	1310	1330		
4.89	J3-9550	1260	1320	1320	1310	
3.10	KOL-7					1380

AJQ, albite-jadite-quartz; GADiS, garnet-anorthite-diopside-silica; GAHdS, garnet-anorthite-hedenbergite-silica; GAHS, garnet-anorthite-hornblende-silica; GODSS, garnet-olivine-diopside-spinel-silica.

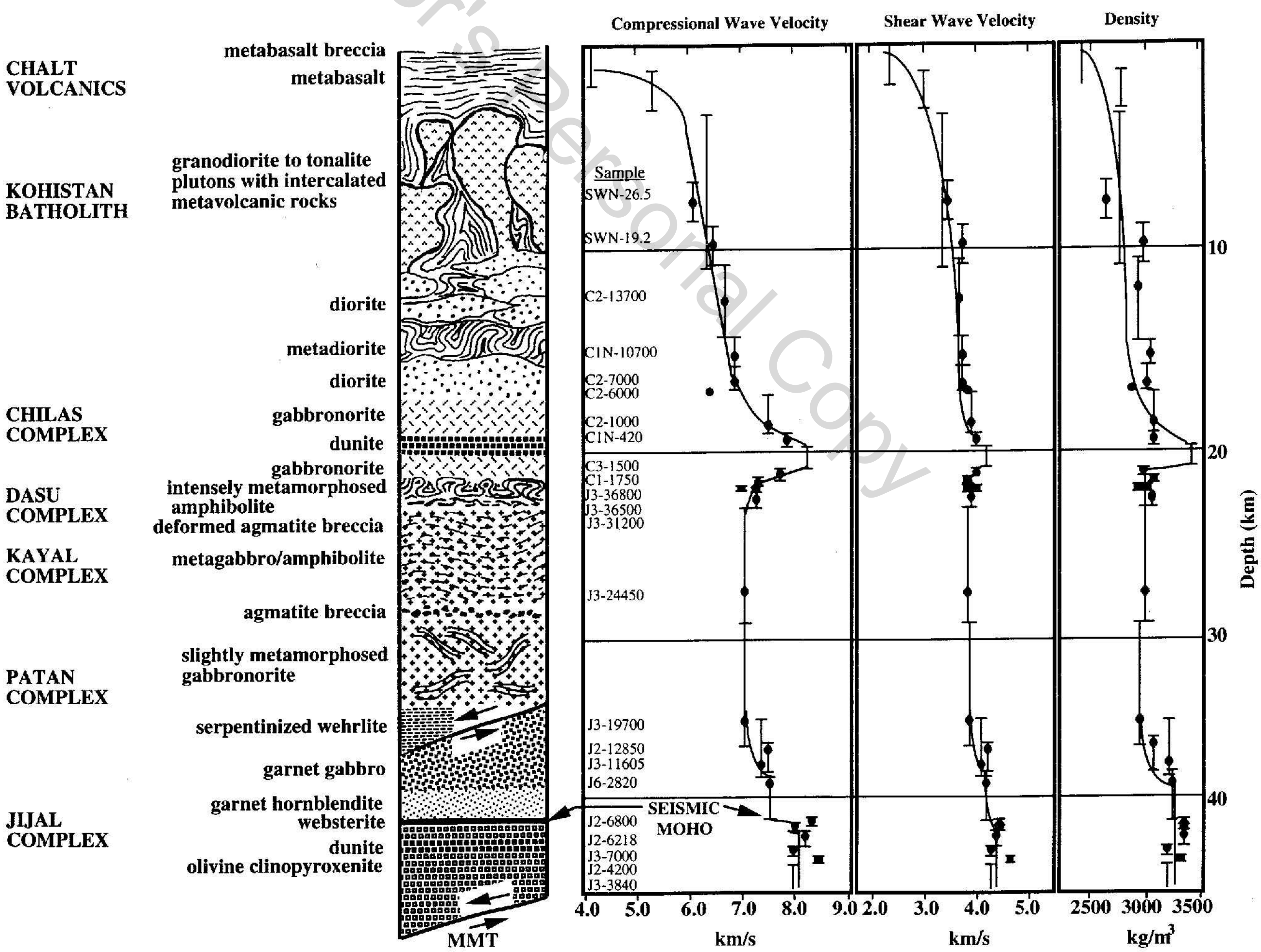

Figure 4. Schematic lithologic column for the Kohistan arc. Also shown are correlated profiles for laboratory-measured *Vp, Vs* and density. Sample stratigraphic locations in the profiles are shown as dots. Brackets through dots indicate intervals represented by each sample. Data for dunite in Chilas Complex is from *Chroston and Simmons* [1989]. Data for uppermost lithologies taken from compilation by N. I. Christensen (unpublished data, 1994) based on the descriptions of *Pudsey* [1986] and *Petterson et al.* [1991a, b].

reconstruction of a new, schematic stratigraphic column for the Kohistan arc (Figure 4). Recognition that the Jijal Complex represents the cumulate base of the arc implies a total thickness of at least 45 km, and equilibration pressures derived from several stratigraphic intervals within the arc enables us to make better constrained interpretations of the velocity structure of the arc than existing models allow. Figure 4 also shows profiles for laboratory-measured *Vp*, *Vs*, and density correlated to the stratigraphic profile generated by this investigation. While in general this profile is remarkably similar in appearance to velocity profiles generated by seismic refraction and/or reflection studies in other continental regions [e.g., *Meissner*, 1986], two striking differences merit consideration. First, the strong inflection in all three profiles at 20 km depth is caused by the presence of a 1-km-thick, high-velocity, high-density dunite cumulate in the Chilas Complex. Local anomalies of this magnitude may be overlooked or deemed insignificant in regional seismic studies. Alternatively, they may be too thin to be resolved by refraction and deep-crustal reflection surveys. However, given the lateral continuity of this unit (in excess of 25 km) we must consider that high-velocity anomalies in other profiles may reflect real changes in lithology which have significant bearing on the composition and evolution of arc crust.

The second and most intriguing fact brought to light in these profiles addresses the strong inflection in *Vp*, *Vs* and density evident at about 40 km depth. Many geoscientists would interpret this sharp change in *Vp* from 7.2 to greater than 8.0 km s^{-1} as representing the transition from the crust into the Earth's mantle [e.g. *James and Steinhart*, 1966]. In this case, however, this inflection is due to the transition from ultramafic cumulates to mafic cumulates in a lower crustal, continuous, coherent layered intrusion. The abrupt change in physical properties coincides with the cumulus arrival of plagioclase in the crystallization sequence of the Jijal Complex. Although the actual crust-mantle boundary has been obscured by the Main Mantle Thrust, we recognize that it must lie at least 4 km farther downsection than might be interpreted from the velocity profile. While a possible discordance between the seismic Moho and the petrologic crust-mantle boundary has been inferred by some researchers (notably *White* [1988] and *Nelson* [1991]), and described for oceanic crust based on ophiolites [*Malpas*, 1978], it has yet to be documented for continental crust. The lowermost

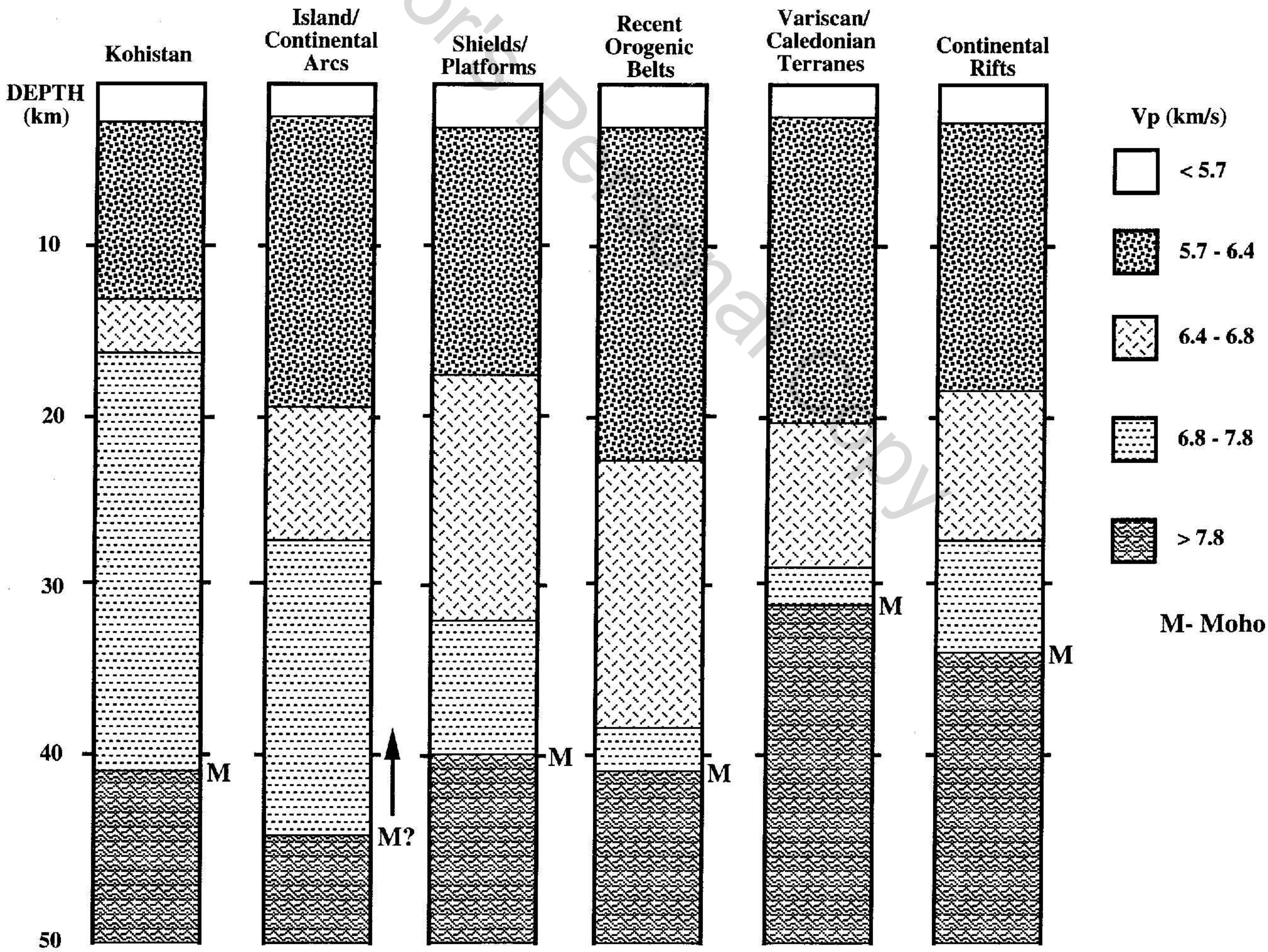

Figure 5. Average seismic velocities of various crustal sections [from *Mooney and Meissner*, 1991] compiled from seismic refraction and/or reflection data. Also shown is a profile with the same divisions in compressional wave velocity derived from laboratory measurements and constrained by our lithostratigraphic column for the Kohistan terrane. The thick, lower-crustal, high-velocity zone from Kohistan lends geophysical corroboration to the interpretation based on structural, geochemical, and mineralogical grounds of the Kohistan terrane as an accreted arc.

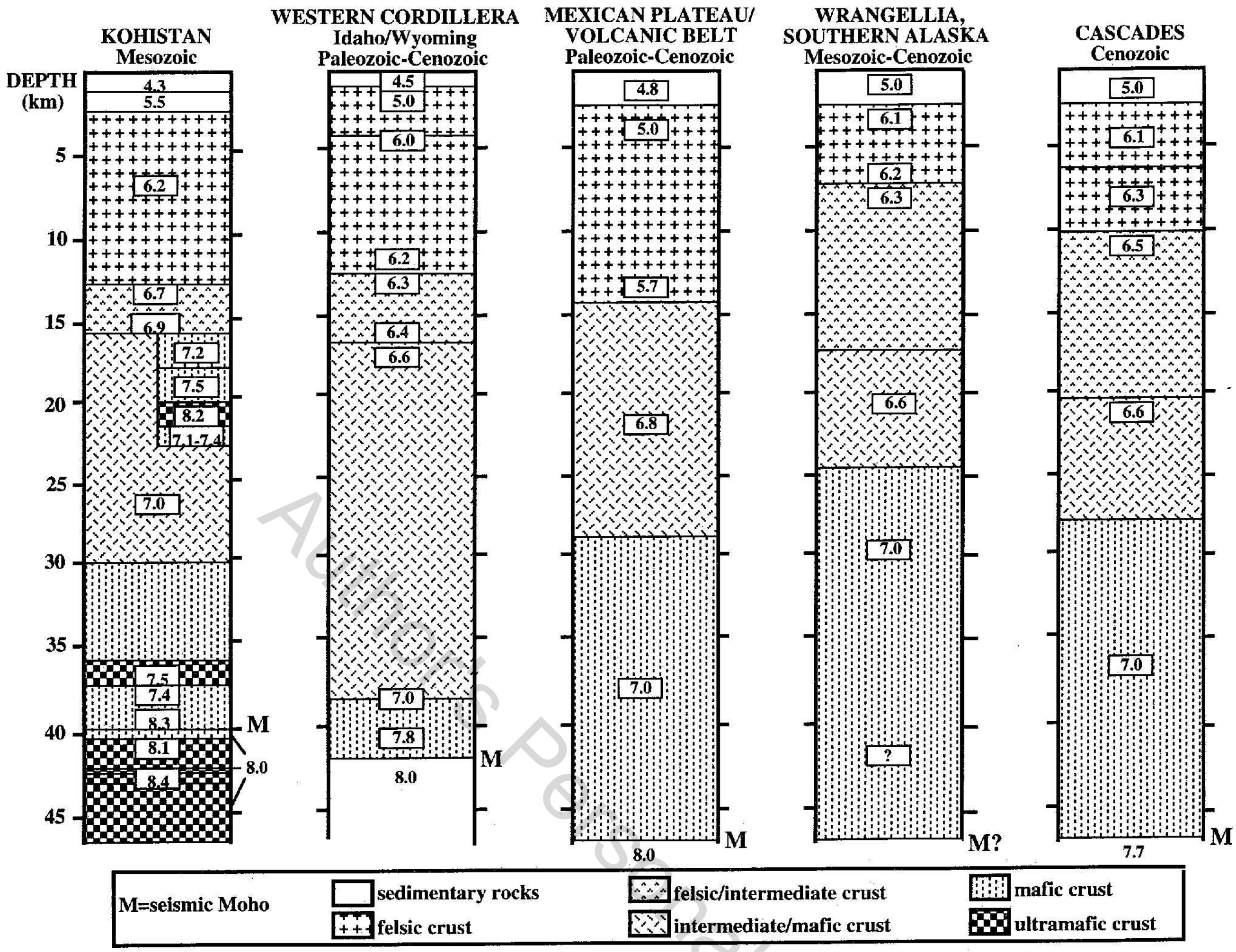

Figure 6. Seismic velocity profiles for various cordilleran terranes [from *Mooney and Braile*, 1989] based on seismic refraction and/or reflection data compared to a profile generated from laboratory measurements for rocks from the Kohistan arc. Average mean Vp for the Cascades, Wrangellia, Western United States, and Kohistan (calculated from unit thickness and mean unit velocities) are virtually indistinguishable at 6.7 plus or minus 0.05 km s^{-1}. Inset in Kohistan profile between 15.5 and 22.5 km depth represents the laboratory-measured variability in samples from the Chilas Complex, superimposed on a thick, homogeneous section of amphibolite.

intrusion in the Kohistan arc terrane (the Jijal Complex) provides one of the few windows into this transition zone. The remarkable preservation of pristine igneous features in the Jijal Complex and, to a lesser degree, in the overlying Patan Complex may well represent our best opportunity to investigate in detail this transition in exposed lower- crustal rocks.

Figure 5 shows average seismic velocities of various crustal sections compiled by *Mooney and Meissner* [1991]. For comparison, we present a profile derived from the laboratory-measured (where available), or compositionally estimated Vp for our lithostratigraphic section from the Kohistan arc. The most distinguishing seismic characteristic of island and continental arcs as opposed to other crustal sections is the presence of a thick, high-velocity lower crustal zone [*Mooney and Meissner*, 1991]. The presence of this zone in the Kohistan profile gives us geophysical corroboration of the interpretation championed by various researchers [*Tahirkheli et al.*, 1980; *Bard et al.*, 1980; *Coward et al.*, 1982] of this terrane as an arc section.

Given this corroboration, comparisons to other accreted arc terranes can be drawn. Figure 6 shows the seismic velocity structure of several different cordilleran terranes, published by *Mooney and Braile* [1989] and derived from seismic refraction and reflection surveys. Also shown is a seismic velocity profile for Kohistan generated from this research. While substantially more detail is apparent in the Kohistan model, the resemblance to the models derived from seismic surveys is striking. The mean crustal Vp (calculated from interval thickness, mean interval Vp, and total crust thickness) for the Cascades, Wrangellia, Western United States, and Kohistan are virtually indistinguishable at 6.70 ± 0.05 km s^{-1}.

A graphic representation of the data from Table 1 is presented in Figure 7. Density increases with depth in the section at approximately 20 kg m^{-3} km^{-1} from 2400 to 3300 kg m^{-3}. Both compressional and shear wave velocities exhibit an increase with increasing pressure. The apparent separation of lithologic units in terms of shear wave velocity in the middle density ranges (grouping of amphibolites, Chilas Complex rocks, and Kohistan batholith rocks) is due to the high quartz content of the amphibolites. Contributing to this shift is the pressure differential invoked for the different stratigraphic units. Quartz content,

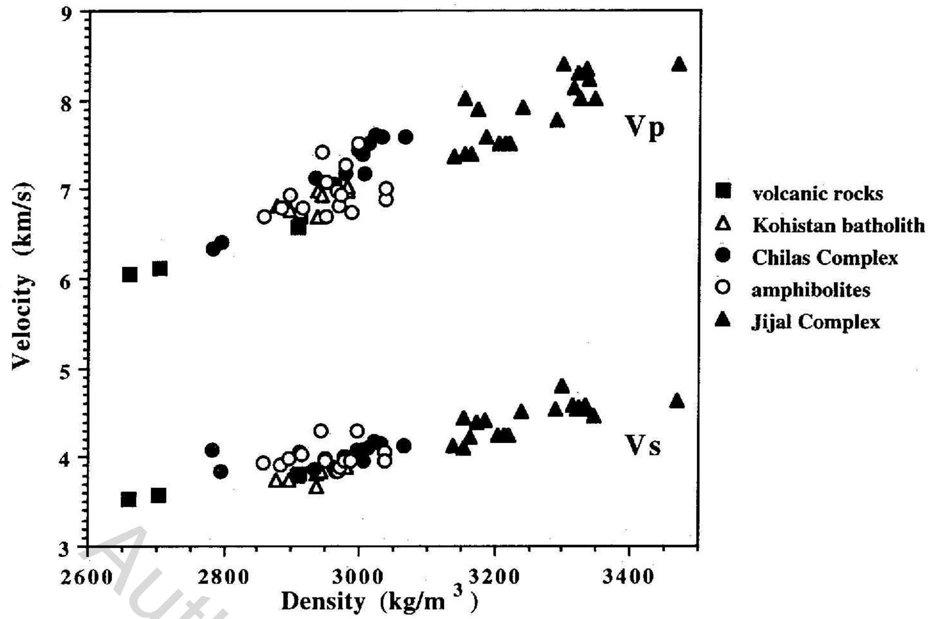

Figure 7. Compressional (*Vp*) and shear (*Vs*) wave velocities plotted against density. Compressional data exhibit expected uniform positive slope with increasing density. Shear wave values allow distinction of quartz-rich and quartz-poorer rock types at equivalent densities.

however, is the dominant control on this behavior, since similar pressure constraints produce no evident lithostratigraphically controlled separation in compressional wave velocity over this same interval. The near coincidence of shear wave velocities, despite different estimated pressures for the mid- to upper-crustal units, is due to the higher percentage of modal quartz in the diorites as compared to the gabbronorite. The fine-grained, quartz-rich chilled margin of the Chilas Complex also exhibits anomalously high shear wave velocity.

Figure 8 examines the variation in primary lithology and stratigraphic interval expressed as the ratio of compressional to shear wave velocity plotted against density. Separations between the stratigraphic intervals is readily apparent in this figure as the groupings suggested by the previous figure are enhanced. Samples from the Chilas Complex, Kohistan batholith and the lower-crustal stacked intrusions all have similar density (2975 ± 50 kg m^{-3}), but distinctly different values for *Vp/Vs*. While the Chilas Complex and the amphibolites equilibrated at roughly equivalent pressures, the abundant quartz present in the latter contributes to elevated shear wave velocity. Again, pressure contributions notwithstanding, the mafic rocks of the Chilas complex rocks can be distinguished from the more evolved diorites of the Kohistan batholith. The interleaved volcanic rocks from the Kohistan batholith exhibit low *Vp* to *Vs* ratios due to the advanced degree of evolution of their parental magmas.

Discussion

A wide variety of methods have been employed to estimate the bulk chemical composition of the Earth's crust. The earliest of these assumed that surficially exposed crystalline basement was representative of the bulk crust [*Clarke*, 1924; *Clarke and Washington*, 1924; *Goldschmidt*, 1933, 1954]. More recent estimates have been based on recognition of the variable contributions from a mafic lower and felsic upper crust [*Poldervaart*, 1955; *Vinogradov*, 1962; *Taylor*, 1964; *Pakiser and Robinson*, 1966; *Ronov and Yaroshevsky*, 1967, 1969; *Galdin*, 1974], on rare earth element constraints (Taylor, 1964), and on combinations of various partial crustal compositions [*Holland and Lambert*, 1972; *Taylor and McLennan*, 1981; *Weaver and Tarney*, 1984a, b]. These estimates, despite the diverse data bases that support them, are remarkably similar (for a review see *Fountain and Christensen* [1989]. Inasmuch as we have whole rock major element chemistry for representative lithologic units from this section and estimates of unit thickness constrained by geobarometry, we can apportion the major element oxides and calculate a bulk composition for the Kohistan arc (Table 6). Table 6 also includes several recent estimates of the bulk chemical composition of continental crust, as well as a similar estimate for the Talkeetna island arc complex from southern Alaska [*Pearcy et al.*, 1990]. The estimated bulk composition of the Kohistan arc (basaltic andesite) is significantly more mafic than previous estimates of the bulk continental crust. However, our estimate is practically identical to the mass balance result of *Pearcy et al.* [1990] for Talkeetna. *Pearcy et al.* [1990] also recognize this discordance despite the contention that a significant portion of the continental crust has been derived by accretion of magmatic arcs onto continental margins. They invoke a combination of delamination of the ultramafic base of arcs, alkali addition by accretion of various alkalic terranes, and partial melting of the lower arc crust to account for this discordance. Alternatively, previous assessments may have underestimated the mafic component of the bulk crust.

The plate tectonic model for crustal evolution suggests three possible sources for the magmas erupted at island arcs, either melting of the subducting eclogitic slab, melting of the mantle wedge trapped between the subducting slab and the overlying crust, or melting of the crust itself. Although each of these is likely to contribute some component to the final product, there is some debate as to the primary operator in the process.

Melting of continental crust, while certainly a factor in altering the composition of preexisting primitive liquids [*Hildreth*

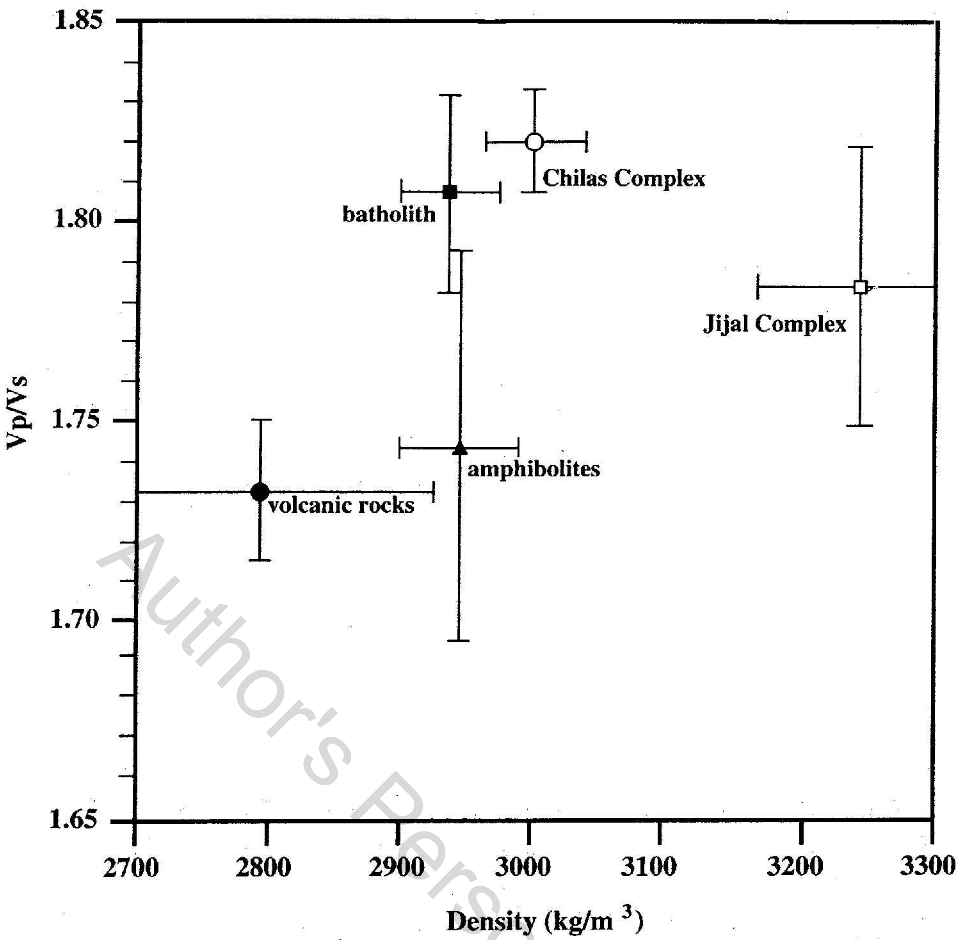

Figure 8. *Vp* divided by *Vs* plotted versus density. Major lithologic units are displayed as mean (symbols) values and standard deviation (error bars). Despite similar densities, midcrustal lithologic units (Chilas, batholith, and amphibolites) can be distinguished due to variability in degree of evolution and metamorphism exhibited as distinct fields of *Vp*/*Vs*. Note that in this representation, sample C2-6000 has not been included in the Chilas Complex average as it imparts an unrealistic bias toward quartz-rich composition (lower *Vp*/*Vs*).

Table 6. Estimates of Bulk Crustal Chemical Composition

	Oxide Wt. %				
	1	2	3	4	5
SiO_2	58.0	63.2	59.0	51.1	51.0
TiO_2	0.8	0.6	1.0	0.7	1.1
Al_2O_3	18.0	16.1	15.2	15.0	15.9
Fe_2O_3	...	...	3.1	...	10.3
FeO	7.5	4.9	3.7	9.5	...
MgO	3.5	2.8	3.5	11.2	8.8
CaO	7.5	4.7	5.1	9.2	9.5
MnO	0.1	0.1	0.1	0.2	0.2
Na_2O	3.5	4.2	3.7	2.5	2.6
K_2O	1.5	2.1	3.1	0.5	0.6
P_2O_5	...	0.2	0.3	0.1	0.2
H_2O	...	...	1.7	...	...

Column heads refer to 1, bulk continental crust [*Taylor and McLennan*, 1981]; 2, bulk continental crust [*Weaver and Tarney*, 1984a]; 3, bulk continental crust (from surface exposures) [*Clarke*, 1924]; 4, Talkneeta arc terrane bulk crust [*Pearcy et al.*, 1990]; and 5, Kohistan arc terrane (this work), bulk crust (Total Fe as Fe_2O_3, FeO equivalent 9.3).

and Moorbath, 1988], is incapable under any plausible circumstance of generating the primitive liquids of the tholeiitic suite associated with young arc magmatism and will not be considered in this discussion. While partial melting of mantle peridotite can account for the tholeiitic series magmas, it does not adequately explain the derivation of the calc-alkaline and high alumina basalt magmas common to many island arcs. In response to this apparent anomaly, some researchers (notably, *Marsh* [1979,1982], *Brophy and Marsh* [1986], *Johnston* [1986], and *Myers et al.* [1986]) have argued that the primary contribution to arc magmas is derived from partial melting of the subducted eclogitic oceanic crust.

The singularly most derisive argument against accepting picritic, mantle-derived parental magmas is that, with minor exceptions, arc basaltic magmas have Mg/Mg+Fe and contents of Ni, Cr, and other elements that cannot represent chemical equilibrium with what are accepted to be upper mantle ultramafic rocks under any conditions that are geophysically relevant [e.g., *Baker and Eggler*, 1983]. In effect, this means either that arc basalts are not derived from peridotitic mantle but rather from some alternative source, or that the compositions of the magmas have undergone significant modification since their derivation in a peridotitic source region.

While models supporting ecologite melting have been able to duplicate rare earth element patterns broadly consistent with typical arc high alumina basalt patterns [*von Drach et al.*, 1986; *Brophy and Marsh*, 1986], other, more persuasive considerations support a picritic parent [*Crawford et al.*, 1987]. It is notable, however, that the parental picrite/olivine tholeiite hypothesis requires that there be voluminous ultramafic cumulates in the lower crust beneath island and continental arcs. A subducted, eclogitic parent effectively precludes the possibility of the development of these cumulates as fractionation of a partial melt of an evolved liquid cannot produce high-magnesia olivine-rich cumulates. In the Jijal Complex, we have recognized a several kilometer thick ultramafic cumulate sequence, emplaced at or near the base of the crust. Any estimate of the bulk composition of the Kohistan arc crust which failed to include this thick ultramafic base would be too silicic.

Given that the Kohistan arc may record the only exposed complete section through the crust of the Earth, we can address the likelihood of this terrane as an analogue for other arcs worldwide. Garnet-bearing gabbro xenoliths have been recovered from volcanic pipes in the Central Sierra Nevadas [*Dodge et al.*, 1988]. *DeBari and Coleman* [1989] describe a unit of garnet gabbro in the lower crustal section from Tonsina, Alaska. *Hamer and Noyes* [1982] report igneous garnet in rocks from an arc setting from the Trinity Peninsula, Antarctica. And *Shevchenko* [1986] documents rare igneous garnet in xenoliths occurring in the volcanic rocks of the Kamchatka arc. The cited reports suggest that igneous garnet may be quite common the lower crust of arc terranes. There is no question that, based on structural, mineralogical, and geochemical evidence, the Kohistan terrane represents a section through an island arc. We have presented geophysical data from the laboratory-measured physical properties of rocks representative of the major lithologies exposed along the lower two-thirds of this section which corroborates this interpretation. We submit that our investigation strongly suggests that the Kohistan terrane represents our most transparent window into the otherwise veiled and enigmatic realm of deep crustal genesis and evolution in island arcs.

Summary and Conclusions

A multidisciplinary approach, including field study, petrology, geochemistry, and physical properties analysis has engendered several new interpretations relevant to the Kohistan arc. The continuity, accessibility, and complexity of this terrane are unparalleled. The superb, nearly continuous exposure, from the ultramafic foundation through the midcrustal mafic complexes, into the evolved, upper crustal plutonics, and ultimately into the supracrustal volcanics, was invaluable in the development of the following conclusions.

1. Geobarometric constraints derived from extensive mineral chemistry analysis, recently published, rigorous activity-composition models, and an internally consistent thermodynamic data base has allowed reconstruction of a new lithologic column for the arc. This column, partially dependent on published accounts for the upper third of the section, indicates a total thickness of the arc in excess of 45 km.

2. Correlation of laboratory measured physical properties with the new stratigraphic column has generated a velocity profile comparable to profiles developed from seismic reflection and refraction studies. The midcrustal, high-velocity zone in our profile is produced by a laterally continuous, thick ultramafic horizon within a layered mafic intrusion, which significantly effects bulk velocity and chemical composition estimates. While units of the order of 1 km thick may be difficult to resolve in seismic refraction and deep-crustal reflection surveys, they may reflect real changes in lithology and merit consideration when encountered.

3. Documentation of the discordance between the seismic discontinuity which could be interpreted to represent the crust-mantle boundary and the actual base of the crust is certainly one of the most significant results of this research. The strong inflection in the velocity profile to greater than 8.0 km s^{-1} is due to the transition from plagioclase-bearing to plagioclase-free cumulate rocks in a continuous ultramafic-mafic intrusion. The base of the crust lies at least 4 km below this transition and is now either obscured by the MMT or has been stripped off during obduction onto the Indian plate.

4. Our profile provides geophysical corroboration to geochemical, mineralogical, and structural studies which recognize the Kohistan terrane as an island arc. This is apparent in the thick, lower crustal, high-velocity zone characteristic of island arcs.

5. Calculation of the mean crustal velocity for this section yields values which are imperceptibly different from similar estimates for other cordilleran arc terranes.

6. The ratio of *Vp* divided by *Vs* is a useful correlative tool for lithologic variability for samples from the Kohistan terrane. High *Vp* to *Vs* values reflect quartz poor lithologies from this sample suite.

7. Geochemical indices of fractionation exhibit reasonable correlation with compressional and shear wave velocities. The differentiation index of *Thornton and Tuttle* [1960] appears to have the strongest correspondence of the indices examined. Since this relationship might not be expected for genetically distinct or intensely altered terranes, its evidence here warrants more detailed investigation to establish whether the small data set is imparting a bias.

8. An estimate of the bulk chemical composition for the Kohistan arc does not compare favorably with published estimates of the bulk composition of continental crust. There is remarkable agreement, however, with a mass balance estimate for the composition of an arc terrane from Alaska, This may support the opinion of *Pearcy et al.* [1990] that simple accretion of magmatic arcs cannot account for the bulk chemical composition of the crust. It is also possible that previous appraisals have underestimated the mafic component of the bulk continental crust, due to exclusion of thick accumulations of ultramafic material at or near the base of the crust.

9. The presence of garnet gabbros at deep crustal levels in other cordilleran terranes suggests that the crustal section interpreted from the Kohistan terrane may be a suitable analogue for active arcs.

Acknowledgments. The field studies were supported by a grant from the National Science Foundation EAR-88-17353 to Robert Loucks, whose contribution to this work is acknowledged and appreciated. The laboratory measurements were supported by the Office of Naval Research contract N-00014-89-J-1209. D.J.M. also received support from the Indiana Mining and Minerals Resources Research Institute grant G1114118. We also wish to acknowledge M. Ashraf and the faculty and staff at Azad Jammu and Kashmir University, Pakistan, for their contribution to this research. This paper benefitted from insightful review and comment from R. Lillie, J. McBride, T. Pratt, and N. Chroston.

References

Baker , D. R., and D. H. Eggler, Fractionation paths of Atka (Aleutian): high alumina basalts constraints from phase relations, *J. Volcanol. Geotherm. Res.*, *8*, 387-404, 1983.

Bard, J. P., H. Maluski, P. Matte, and F. Proust, The Kohistan sequence, crust and mantle of an obducted island arc, *Geol. Bull. Univ. Peshawar*, *13*, 87-94, 1980.

Berman, R. G., Mixing properties of Ca-Mg-Fe-Mn garnets, *Am. Mineral.*, *75*, 328-344, 1990.

Birch, F., The velocity of compressional waves in rocks to 10 kilobars, *J. Geophys. Res.*, *65*, 1083-1102, 1960.

Birch, F., Composition of the Earth's crust, *Geophys. J.*, *4*, 295-311, 1961.

Blundy, J. D., and T. J. B. Holland, Calcic amphibole equilibria and a new amphibole-plagioclase geothermometer, *Contrib. Mineral. Petrol.*, *104*, 208-224, 1990.

Brey, G. P., and T. Köhler, Geothermometry in four phase lherzolites, II, New thermobarometers, and practical assessment of existing thermobarometers, *J. Petrol.*, *31*, 1353-1378, 1990.

Brophy, J. G., and B. D. Marsh, On the origin of high alumina arc basalt and the mechanics of melt extraction, *J. Petrol.*, *27*, 763-785, 1986.

Carroll, M. R., and P. J. Wyllie, Experimental phase relations in the system tonalite-peridotite-H_2O at 15 kbar: Implications for assimilation and differentiation processes near the crust-mantle boundary, *J. Petrol.*, *30*, 1351-1382, 1989.

Carroll, M. R., and P. J. Wyllie, The system tonalite-H_2O at 15 kbar and genesis of calc-alkaline magmas, *Am. Mineral.*, *75*, 345-357, 1990.

Christensen, N. I., Compressional wave velocities in rocks at high temperatures and pressures, critical thermal gradients, and crustal low velocity zones, *J. Geophys. Res.*, *84*, 6849-6877, 1979.

Christensen, N. I., Seismic velocities, in *Handbook of Physical Properties of Rocks*, vol. 2, edited by R. S. Carmichael, pp. 1-226, CRC Press, Boca Raton, Fla., 1982.

Christensen, N. I., Measurements of dynamic properties of rock at elevated temperatures and pressures, in *Measurement of Rock Properties at Elevated Pressures and Temperatures*, edited by H. J. Pincus and E. R. Hoskins, pp. 93-107, American Society for Testing and Materials, Philadelphia, Pa., 1985.

Christensen, N. I., Reflectivity and seismic properties of the deep continental crust, *J. Geophys. Res.*, *94*, 17793-17804,1989.

Christensen, N. I., and D. L. Szymanski, Seismic properties and the origin of reflectivity from the Brevard fault zone, *J. Geophys. Res.*, *93*, 1087-1102, 1988.

Chroston, P. N., and G. Simmons, Seismic velocities from the Kohistan Volcanic Arc, northern Pakistan, *J. Geol. Soc. London*, *146*, 971-979, 1989.

Clarke, F. W., The data of geochemistry, *U.S. Geol. Surv. Bull.*, *770*, 1924.

Clarke, F. W., and H.S. Washington, The composition of the Earth's crust, *U.S. Geol. Surv. Prof. Pap.*, *127*, 1924.

Coward, M. P., M. Q. Jan, D. Rex, J. Tarney, M. Thirwall, and B. F. Windley, Geotectonic framework of the Himalaya of northern Pakistan, *J. Geol. Soc. London*, *139*, 299-308, 1982.

Coward, M. P., B. F. Windley, R. D. Broughton, I. W. Luff, M. G. Petterson, C. J. Pudsey, D. C. Rex, and M. A. Kahn, Collision tectonics in the NW Himalayas, in Collision Tectonics, edited by M. P. Coward and A. C. Ries, *Geol. Soc. Spec. Publ. London*, *19*, 203-219, 1986.

Cox, R. G., J. D. Bell, and R. J. Pankhurst, *The Interpretation of Igneous Rocks*, 30-45, Allen and Unwin, Winchester, Mass., 1979.

Crawford , A. J., T. J. Falloon, and S. Eggins, The origin of island arc high-aluminum basalts, *Contrib. Mineral. Petrol.*, *97*, 417-430, 1987.

DeBari, S. M., and R. G. Coleman, Examination of the deep levels of an island arc: Evidence from the Tonsina ultramafic-mafic assemblage, Tonsina, Alaska, *J. Geophys. Res.*, *94*, 4373-4391, 1989.

Dodge, F. C. W., J. P. Lockwood, and L. C. Calk, Fragments of the mantle and crust from beneath the Sierra Nevada batholith: Xenoliths in a volcanic pipe near Big Creek, California, *Geol. Soc. Am. Bull.*, *100*, 938-947, 1988.

Elkins, L. T., and T. L. Grove, Ternary feldspar experiments and thermodynamic models, *Am. Mineral.*, *75*, 544-559, 1990.

Fountain, D. M., and N. I. Christensen, Composition of the continental crust and upper mantle; A review, in Geophysical Framework of the Continental United States, edited by L. C. Pakiser and W. D. Mooney, *Mem. Geol. Soc. Am.*, *172*, 711-742, 1989.

Galdin, N. E., Composition of crust in the ancient shields, *Geochem. Int.*, *11*, 270-281, 1974.

Goldschmidt, V. M., Grundlagen der quantitativen Geochemie, *Fortschr. Mineral. Kristallogr. Petrogr.*, *17*, 112-156, 1933.

Goldschmidt, V. M., *Geochemistry*, 11-26, Clarendon, Oxford, 1954.

Graham, C. M., and R. Powell, A garnet-hornblende geothermometer; calibration, testing and application to the Pelona Schist, Southern California, *J. Metamorph. Geol.*, *2*, 13-31, 1984.

Hakli, T. A., and T. L. Wright, The fractionation of nickel between olivine and augite as a geothermometer, *Geochim. Cosmochim. Acta*, *31*, 877-884, 1967.

Hamer, R. D., and A. B. Noyes, Composition and origin of garnet from the Antarctic Peninsula Volcanic Group of Trinity Peninsula, *J. Geol. Soc. London*, *139*, 713-720, 1982.

Hamilton, W. B., Plate tectonics and island arcs, *Geol. Soc. Am. Bull.*, *100*, 1503-1527, 1988.

Hildreth, W., and S. Moorbath, Crustal contribution to arc magmatism in the Andes of central Chile, *Contrib. Mineral. Petrol.*, *98*, 455-489, 1988.

Holland, J. G., and R. St. J. Lambert, Major element chemical composition of shields and the continental crust, *Geochim. Cosmochim. Acta*, *36*, 673-683, 1972.

Holland, T. J. B., Activities of components in omphacitic solid solutions, an application of Landau theory to mixtures, *Contrib. Mineral. Petrol.*, *105*, 446-453,1990.

Holland, T. J. B., and R. Powell, An enlarged and updated internally consistent thermodynamic dataset with uncertainties and correlations: The system K_2O-Na_2O-CaO-MgO-MnO-FeO-Fe_2O_3-Al_2O_3-TiO_2-SiO_2-C-H_2-O_2, *J. Metamorph. Geol.*, *8*, 89-124, 1990.

James, D. E. and J. S. Steinhart, Structure beneath the continents: a critical review of explosion studies 1960-1965, in *The Earth Between the Continents A Volume of Geophysical Studies in Honor of Merle A. Tuve*, *Geophys. Monogr. Ser.*, vol. 10, edited by J. S. Steinhart and T. J. Smith, 293-333, AGU, Washington, D. C.,1966.

Jan, M. Q., and M. Asif, Geochemistry of tonalites and quartz diorites of the Kohistan-Ladakh (Transhimalayan) granitic belts in Swat N. Pakistan, in *Granites of Himalayas, Karakoram and Hindu Kush*, edited by F. A. Shams, pp. 355-376, University of Punjab, Institute of Geology, Lahore, Pakistan, 1983.

Jan, M.Q., and R.A. Howie, The mineralogy of the metamorphosed basic and ultrabasic rocks of the Jijal Complex, Kohistan, NW Pakistan, *J. Petrol.*, *27*, 85-126, 1981.

Johnston, A.D., Anhydrous P-T relations of near-primary high alumina basalts from the South Sandwich Islands: Implications for the origin of island arcs and tonalite-trondjemite series rocks, *Contrib. Mineral. Petrol.*, *92*, 368-382, 1986.

Krogh, E. J., The garnet-clinopyroxene Fe-Mg geothermometer - A reinterpretation of existing experimental data, *Contrib. Mineral. Petrol.*, *99*, 44-48, 1988.

LeMaitre, R. W., The chemical variability of some common igneous rocks, *J. Petrol.*, *17*, 589-637, 1976

Loucks, R. R., D. J. Miller, M. Ashraf, M. A. Awan, and M. S. Kahn, The Jijal Complex: Layered mafic-ultramafic arc cumulates from the crust-mantle boundary, Pakistani Himalayas (Abstract), *Eos Trans. AGU*, *71*, 664, 1990.

Malpas, J., Magma generation in the upper mantle, field evidence from ophiolitic suites, and application to the generation of oceanic lithosphere, *Philos. Trans. R. Soc. London, Ser. A*, *288*, 527-546, 1978.

Marsh, B. D., Island arc development, some observations, experiments, and speculations, *J. Geol.*, *87*, 687-713, 1979.

Marsh, B.D., The Aleutians, in *Andesites*, edited by R.S. Thorpe, pp. 99-114, John Wiley, New York, 1982.

Meissner, R., *The Continental Crust*, pp. 315, Academic, San Diego, Calif., 1986.

Miller, D. J., R. R. Loucks, and M. Ashraf, Platinum-group element mineralization in the Jijal layered ultramafic- mafic complex, Pakistani Himalayas, *Econ. Geol.*, *86*, 1093-1102, 1991.

Mooney, W. D., and L. W. Braile, The seismic structure of the continental crust and upper mantle of North America, in *The Geology of North America-An Overview*, edited by A. W. Bally and E. R. Palmer, pp. 39-52, Geological Society of America, Boulder, Colo., 1989.

Mooney, W. D., and R. Meissner, Continental crustal evolution observations, *Eos Trans. AGU*, *72*, 537-541, 1991.

Myers, J. D., B. D. Marsh, and A. K. Sinha, Geochemical and strontium isotope characteristics of parental Aleutian arc magmas: Evidence from the basaltic lavas of Atka, *Contrib. Mineral. Petrol.*, *94*, 1-11, 1986.

Nelson, K. D., A unified view of craton evolution motivated by recent deep seismic reflection and refraction results, *Geophys. J. Int.*, *105*, 25-35, 1991.

Pakiser, L. C., and R. Robinson, Composition and evolution of the continental crust as suggested by seismic observations, *Tectonophysics*, *3*, 547-557, 1966.

Pearcy, L. G., S. M. DeBari, and N. H. Sleep, Mass balance calculations for two sections of island arc crust and implications for the formation of continents, *Earth Planet. Sci. Lett.*, *96*, 427-442, 1990.

Petterson, M. G., B. F. Windley, and I. W. Luff, The Chalt Volcanics, N. Pakistan: High Mg tholeiite and low Mg calc-alkaline volcanism in a Cretaceous island arc, *Phys. Chem. Earth*, *17*, 19-30, 1991a.

Petterson, M. G., B. F. Windley, and M. Sullivan, A petrological, chronological, structural, and geochemical review of Kohistan batholith and its relationship to regional tectonics, *Phys. Chem. Earth*, *17*, 47-70, 1991b.

Poldervaart, A., Chemistry of the Earth's crust, *Spec. Pap. Geol. Soc. Am.*, *62*, 119-144, 1955.

Pudsey, C. J., The Northern Suture, Pakistan: Margin of a Cretaceous island arc, *Geol. Mag.*, *123*, 405-423, 1986.

Ronov, A. B. and A. A. Yaroshevsky, Chemical structure of the Earth's crust, *Geochem. Int.*, *4*, 1041-1075, 1967.

Ronov, A. B., and A. A. Yaroshevsky, Chemical composition of the Earth's crust, in *The Earth's Crust and Upper Mantle, Geophys. Monogr. Ser.*, vol. 13, edited by P. J. Hart, pp. 37-57, AGU, Washington, D. C., 1969.

Shevchenko, Y., Composition of minerals of some magmatic rocks of the Kuril-Kamchatka island arc, *Sov. Geol. Geophys. Engl. Transl.*, *27*, 52-61, 1986.

Tahirkheli, R. A. K., M. Mattauer, F. Proust, and P. Tapponier, The India-Eurasia suture zone in northern Pakistan: Synthesis and interpretation of recent data at plate scale, in *Geodynamics of Pakistan*, edited by A. Farah and K. A. DeJong, pp. 125-130, Geological Survey of Pakistan, Quetta, 1980.

Taylor, S. R., Abundance of chemical elements in the continental crust: A new table, *Geochim. Cosmochim. Acta*, *28*, 1273-1286, 1964.

Taylor, S. R., and S. M. McLennan, The composition and evolution of the continental crust: rare earth element evidence from sedimentary rocks, *Phil. Trans. R. Soc. London, Ser. A*, *301*, 381-399, 1981.

Thornton, C. P., and O. F. Tuttle, Chemistry of igneous rocks: I. Differentiation index, *Am. J. Sci.*, *258*, 664-684, 1960.

Treloar, P. J., K. H. Brodie, M. P. Coward, M. Q. Jan, M. A. Khan, R. J. Knipe, D. Rex, and M. P. Williams, The evolution of the Kamila shear zone, in *Exposed Cross-Sections of the Continental Crust*, edited by M. H. Salisbury and D. M. Fountain, pp. 175-214, Kluwer Academic,Hingham, Mass., 1990.

Varma, A., CRC *Handbook of Inductively Coupled Plasma Atomic Emission Spectroscopy*, CRC Press, Boca Raton, Fla., 1991.

Vinogradov, A. P., Average contents of chemical elements in the principal types of igneous rocks of the Earth's crust, *Geochemistry*, *7*, 641-664,1962.

von Drach, V., B.D. Marsh, and G. J. Wasserburg, Nd and Sr isotopes in the Aleutians: Multicomponent parenthood of island arc magmas, *Contrib. Mineral. Petrol.*, *92*, 13-34, 1986.

Weaver, B. L., and J. Tarney, Major and trace element composition of the continental lithosphere, in *Structure and Evolution of the Continental Lithosphere*, edited by H. N. Pollack and V. R. Murthy, 39-68, Pergamon, New York, 1984a.

Weaver, B. L., and J. Tarney, Empirical approach to estimating the composition of the continental crust, *Nature*, *310*, 575-577, 1984b.

White, R. S., The Earth's crust and lithosphere, in *Oceanic and Continental Lithosphere; Similarities and Differences*, edited by M. A. Menzies and K. G. Cox, *J. Petrol. Spec. Issue*, *29*, 1-10, 1988.

N.I. Christensen, Department of Earth and Atmospheric Sciences, Purdue University, West Lafayette, IN 47907. (e-mail: chris@gphys1.geo.purdue.edu)

D.J. Miller, Ocean Drilling Program, TAMU Research Park, 1000 Discovery Drive, College Station Station, TX 77845.

(Received April 29, 1993; revised October 28, 1993; accepted January 5, 1994.)